Agenzia nazionale per le nuove tecnologie,
l'energia e lo sviluppo economico sostenibile

MINISTERO DELLO SVILUPPO ECONOMICO

Ricerca di Sistema elettrico

Test di caratterizzazione sperimentale del sistema per la rilevazione di piccole perdite nel Generatore di Vapore LFR

M. Eboli, D. Mazzi, F. Giannetti, T. Stella, A. Del Nevo, A. Neri
S. Cati, D. Gianotti, M. Valdiserri, D. Santoli

Report RdS/PAR2017/119

Test di caratterizzazione sperimentale del sistema per la rilevazione di piccole perdite nel Generatore di Vapore LFR

M. Eboli (Università di Pisa), D. Mazzi (SRS), F. Giannetti (Sapienza Università di Roma) T. Stella (ISE),
A. Del Nevo, A. Neri, S. Cati, D. Gianotti, M. Valdiserri, D. Santoli (ENEA)

Settembre 2018

Report Ricerca di Sistema Elettrico

Accordo di Programma Ministero dello Sviluppo Economico - ENEA
Piano Annuale di Realizzazione 2017
Area: Generazione di Energia Elettrica con Basse Emissioni di Carbonio
Progetto: Sviluppo competenze scientifiche nel campo della sicurezza nucleare e collaborazione ai programmi internazionali per il nucleare di IV Generazione.
Linea: Collaborazione ai programmi internazionali per il nucleare di IV Generazione
Obiettivo: Progettazione di sistema e analisi di sicurezza
Responsabile del Progetto: Mariano Tarantino, ENEA

Titolo

Test di caratterizzazione sperimentale del sistema per la rilevazione di piccole perdite nel Generatore di Vapore LFR

Descrittori

Tipologia del documento: Rapporto Tecnico

Collocazione contrattuale: Accordo di programma ENEA-MSE su sicurezza nucleare e reattori di IV generazione

Argomenti trattati: Generation IV reactors, Tecnologia del piombo, Sicurezza Nucleare

Sommario

Relativamente alla caratterizzazione sperimentazione dei generatori di vapore, uno dei principali problemi di sicurezza del progetto di reattore nucleare refrigerato a metallo liquido è la rottura dei tubi del generatore di vapore. Infatti, tale evento può implicare la propagazione di un'onda di pressione nel vessel principale che può causare, direttamente o indirettamente, il danneggiamento di strutture interne al vessel del primario. In caso di grandi o piccole perdite, il vapore rilasciato dal secondario del reattore, a pressione più elevata, può essere trascinato dal flusso principale verso l'ingresso del core, causando inserzioni di reattività. Un altro aspetto rilevante è il fatto che tale evento potrebbe avere un impatto sul sistema di controllo della chimica del refrigerante primario, compromettendone l'affidabilità ed il buon funzionamento. Lo sviluppo di un sistema capace di identificare in tempo la presenza di una piccola rottura nel tubo del generatore di vapore potrebbe essere utilizzata per prevenire il degradare della piccola perdita in SGTR: quindi diminuire la probabilità di quello che è, ad oggi, considerato l'incidente di riferimento per la sicurezza del reattore LFR. Nell'ambito dell'attività PAR 2017 in sinergia con il progetto europeo MAXSIMA, sono stati effettuati test sperimentali per caratterizzare il rilascio attraverso tipiche cricche che possono verificarsi nei tubi pressurizzati di un generatore di vapore, e correlare il tasso di rilascio a segnali rilevati da microfoni, accelerometri ed emettitori acustici.

Note

Autori: M. Eboli (Università di Pisa), D. Mazzi (SRS), F. Giannetti (Sapienza Università di Roma), T. Stella (ISE), A. Del Nevo, A. Neri, S. Cati, D. Gianotti, M. Valdiserri, D. Santoli (ENEA)

Copia n. **In carico a:**

1			**NOME**			
			FIRMA			
0	**EMISSIONE**	**23.11.18**	**NOME**	M. Eboli	M. Tarantino	M. Tarantino
			FIRMA	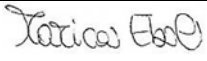		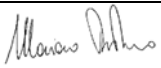
REV.	**DESCRIZIONE**	**DATA**		**REDAZIONE**	**CONVALIDA**	**APPROVAZIONE**

Summary

With regard to the experimental characterization of steam generators in heavy liquid metal cooled reactor, one of the main safety problems for the design is the rupture of the steam generator tubes. During the SGTR event high pressure water enters in the low pressure liquid metal pool in which it rapidly evaporates. The consequent sudden increase of the water specific volume entails pressure waves propagation and cover gas pressurization, which could affect the structural integrity of the surrounding components. Moreover, the rupture of a single SG tube could affect, in principle, the integrity of the neighboring tubes (domino effect), making worse the consequences of the accident scenario. Besides the damaging of the internal structures, a SGTR event could potentially induce an insertion of positive reactivity into the system or reduced cooling efficiency due to steam dragging into the core. It will also have an effect on the chemistry control of the cooling. These consequences may compromise the safety and the reliability of the system.

The development of a system able to promptly detect the presence of a crack in the steam generator tube could be used to prevent the degradation of the small leak in SGTR: therefore decreasing the probability of what is, currently, considered the reference accident for the safety of the LFR reactor. In the framework of PAR 2017 activity in synergy with the European project MAXSIMA, experimental tests have been carried out to characterize the leakage through typical cracks that can occur in the pressurized tubes of a steam generator, and to correlate the release rate to signals detected by microphones, accelerometers and acoustic emission sensor.

List of Revisions

Revision	Date	Scope of revision	Page
0	23/11/2018	First issue	65

List of contents

Summary 2
List of Revisions....3
List of contents....4
List of Figures 5
List of Tables 7
List of Abbreviations 8
1 Introduction....9
2 LIFUS5/Mod3 facility....10
2.1 Test matrix....10
2.2 Objectives of the experimental campaign 10
2.3 Facility description 13
2.4 Injection line....15
2.5 Injection system 15
2.6 Injector device....15
2.7 Installed Components 16
2.8 Detection System: Real Time Data Acquisition For Acoustic Sensors....16
2.8.1 PCB 130E20 16
2.8.2 PCB 377B26 16
2.8.3 Acquisition system hardware....16
2.9 Detection System: Accelerometers And Acoustic Emission Sensor 18
2.9.1 Wilcoxon Research model 786-500 18
2.9.2 IMI Sensor Series EX600B13....18
2.9.3 HOLROYD Instruments 24/7 Ultraspan 19
2.9.4 Multichannel acquisition system....19
3 Description and analysis of Test C1.1_60 40
3.1 Time schedule of test execution 40
3.2 The micro-holed injector and its characterization....40
3.2.1 Geometrical characterization....40
3.2.2 Experimental characterization prior to test 40
3.2.3 RELAP5/Mod3.3 characterization prior to test 40
3.3 Analysis of the Test C1.1_60 and of the leak detection systems data 42
3.3.1 Thermal-hydraulic data analysis and interpretation....42
3.3.2 Analysis of acoustic detection system data and interpretation 52
3.3.3 Analysis of the accelerometers and acoustic emission sensors data and interpretation....60
4 Conclusions....64
List of references 65

List of Figures

Fig. 1 - 3D drawing of LIFUS5/Mod3 with S1B and S1A identification. 23
Fig. 2 – LIFUS5/Mod3 synoptic. 24
Fig. 3 – View of S1A flange penetrations 25
Fig. 4– S1A bottom flange and injection system. 26
Fig. 5 – S2V and level measurement systems. 27
Fig. 6 – S2V system geometry. 28
Fig. 7 – Level measurement system geometry. 28
Fig. 8 – S4A storage tank. 29
Fig. 9 – S3V dump tank. 29
Fig. 10 – Water injection line. 30
Fig. 11 – Sketch of water injection line. 31
Fig. 12 – Sketch of the injection system and main dimensions. 32
Fig. 13 – Injector system device. 33
Fig. 14 – Microphones layout on the top flange of LIFUS5/Mod3 facility. 34
Fig. 15 – PCB 130E20 microphone. 34
Fig. 16 – PCB 377B26 microphone. 35
Fig. 17 – Cooling system assembly. 35
Fig. 18 – Details of the ceramic support (top and bottom view). 35
Fig. 19 – Assembly of the microphone and the Ar cooling system on LIFUS5/Mod3 top flange. 36
Fig. 20 – Penetrations of S1_A top flange and installation inside the vessel. 36
Fig. 21 – Layout of HSA sensor. 37
Fig. 22 – Layout of HTA sensor. 37
Fig. 23 – Layout of AE sensor. 38
Fig. 24 – Multichannel acquisition system DEWESOFT-SIRIUS®. 38
Fig. 25 – Software DEWESOFT X2SP10 for acquisition and data processing. 39
Fig. 26 – Characteristics of N°21 micro-holed injector plate. 45
Fig. 27 – Characterization of orifice N°21 prior to test: S2V level and mass flow rate. 46
Fig. 28 – Characterization of orifice N°21 prior to test: S2V level and calculated integral mass. 46
Fig. 29 – RELAP5/Mod3 nodalization of LIFUS5/Mod3 injection line 47
Fig. 30 – Orifice N°21: calculation of the Ar and H_2O mass flow rate through the orifice at P=1.9 MPa and fluid temperatures between 15-275°C 47
Fig. 31 – Orifice N°21: calculation of the Ar and H_2O integral mass injected through the orifice at P=1.9 MPa and fluid temperatures between 15-275°C 48
Fig. 32 – Test C1.1_60, valve VP-S2L-07, VP-S2L-08 and VE-S2V-05 positions. 49
Fig. 33 – Test C1.1_60, valve VP-S2L-07 and S1A low level positions. 49
Fig. 34 – Test C1.1_60, continuum level in S4A and low level in S1A. 49
Fig. 35 – Test C1.1_60, mass flow rate in injection line and LBE level in S4A time trends. 50
Fig. 36 – Test C1.1_60, mass flow rate in injection line and water level in S2V time trends. 50
Fig. 37 – Test C1.1_60, temperature time trends in the interaction vessel. 50
Fig. 38 – Test C1.1_60, temperature time trends in injection line. 51
Fig. 39 – Test C1.1_60, pressure and temperature time trends in injection line. 51

Fig. 40 – Test C1.1_60, water level in S2V and integral value of injected water time trends. 51
Fig. 41 – Test C1.1_60, raw data channel 1 [time domain]. 53
Fig. 42 – Test C1.1_60, raw data channel 2 [time domain]. 53
Fig. 43 – Test C1.1_60, raw data channel 3 [time domain]. 54
Fig. 44 – Test C1.1_60, raw data channel 4 [time domain]. 54
Fig. 45 – Test C1.1_60, raw data channel 5 [time domain]. 55
Fig. 46 – Test C1.1_60, FFT computing procedure. 56
Fig. 47 – Test C1.1_60, FFT energies file with reported the slice. 57
Fig. 48 – Test C1.1_60, details without bubble @time 17:30:06,50 on channel 1. 58
Fig. 49 – Test C1.1_60, details with a bubble tag @time 17:30:07,02 on channel 1. 59
Fig. 50 – Test C1.1_60, HTA, HSA, AE time RMS trends. 61
Fig. 51 – Test C1.1_60, HTA, HSA, AE time PEAK trends. 61
Fig. 52 – Test C1.1_60, HTA, HSA, AE time RMS trends. 62
Fig. 53 – Test C1.1_60, HTA, HSA, AE time RMS trends. 62
Fig. 54 – Test C1.1_60, HTA, HSA, AE time RMS trends. 63

List of Tables

Tab. 1 – LIFUS5/Mod3 experimental campaign – C series (from September 2017 to April 2018).....11
Tab. 2 – LIFUS5/Mod3 experimental camping – Synoptic and leak detection system acquisition.....12
Tab. 3 – LIFUS5/Mod3: tanks features. 20
Tab. 4 – LIFUS5/Mod3: S1A flange penetrations. 20
Tab. 5 – Valves/Pressure reducers list. 20
Tab. 6 – Installed heating wires. 22
Tab. 7 – Test C1.1_60, time schedule of test execution. 44

List of Abbreviations

ADS	Acoustic Detection System
AE	Acoustic Emission
BIC	Boundary and Initial Conditions
CR	Research Center (in Italian)
DACS	Data Acquisition and Control System
DEGB	Double Ended Guillotine Break
EC	European Commission
EDTAR	Experimental Data and Test Analysis Report
EII	European Industrial Initiative
ELFR	European Lead Fast Reactor
ELSY	European Lead-cooled System
ENEA	Agenzia nazionale per le nuove tecnologie, l'energia e lo sviluppo sostenibile
EoI	End of Injection
EoT	End of Transient
EU	European Union
FP	Framework Program
HLM	Heavy Liquid Metal
HLMFR	Heavy Liquid Metal Fast Reactor
HSA	High Sensitivity Accelerometer
HTA	High Temperature Accelerometer
LBE	Lead Bismuth Eutectic
LEADER	Lead Cooled Advanced Demonstrator Reactor
LFR	Lead Fast Reactor
LV	Level
NA	Not available
NI	Not identified
PC	Absolute Pressure Transducers
PT	Fast Pressure Transducers
S1V	S1 Vessel
S2L	S2 Injection Line
S2V	S2 Vessel
S3L	S3 Discharge Line
S3V	S3 Vessel
SG	Strain Gage
SGTR	Steam Generator Tube Rupture
SNETP	Sustainable Nuclear Energy Technology Platform
SoI	Start of Injection
SoT	Start of Transient
SRA	Strategic Research Agenda
STSG	Spiral Tube Steam Generator
TC	ThermoCouple
THINS	Thermal-Hydraulic of Innovative Nuclear System
TM	Test Matrix

1 Introduction

The new generation Heavy Liquid Metal Fast Reactors (HLMFRs) and Accelerator Driven Systems (ADSs) are currently designed as pool type reactor, implementing the Steam Generators (SGs) or Primary Heat exchangers (PHXs) into the primary pool, where also the core, primary pumps and main components are set. This design feature allows increasing the reactor performance and simplifying the whole layout, by the complete removal of intermediate circuit. In such configuration, the secondary coolant (water), flowing in the heat exchanger tube bundle, at high pressure and subcooled conditions, could come into contact with the primary heavy liquid metal coolant, at higher temperature and lower pressure, in a hypothetical Steam Generator Tube Rupture (SGTR) accident.

During the SGTR event, high pressure water enters in the low pressure liquid metal pool and rapidly evaporates. The consequent sudden increase of the water specific volume entails pressure waves propagation, which could affect the structural integrity of the surrounding components, and cover gas pressurization. Moreover, the rupture of a single SG tube could affect, in principle, the integrity of the neighboring tubes (domino effect), making worse the consequences of the accident scenario. Besides the damaging of the internal structures (HX tube bundle, above core structures, FA, CR, etc..), a SGTR event could potentially induce an insertion of positive reactivity into the system or reduced cooling efficiency due to steam dragging into the core. It will also have an effect on the chemistry control of the cooling. These consequences may compromise the safety and the reliability of the system.

Instrumentation able to promptly detect the presence of a crack in the HX's tube may be used to prevent its further propagation which would possibly lead to a full rupture of the tube. Indeed, the application of the leak before break concept is relevant for improving the safety of a reactor system. In particular, it decreases the probability of the pipe break event. Therefore, early detection might be applied, if endorsed as a technically justifiable approach, for making the consequences of a postulated accident acceptable, or even for eliminating the accident (i.e. in this case the SGTR scenario) altogether.

The report describes one of the tests executed to characterize the leak rate and bubbles sizing through typical cracks occurring in the pressurized tubes. Water at about 20 bar and 200°C was injected into Lead Bismuth Eutectic alloy (LBE). The injection was performed through a laser micro-holed plate.

This experimental analysis aimed to provide engineering feedbacks to promptly detect the presence of a crack in the HX's tube, which may be used to prevent its further propagation. The results of flow rates of the leakage through the selected crack are correlated to signals detected by proper transducers. Different instrumentations are installed and tested in the experimental campaign. Moreover, the acquired experimental data can be used for the validation of numerical models and calculation codes.

2 LIFUS5/Mod3 facility

LIFUS5 is an experimental facility installed at ENEA CR Brasimone. It is designed to be operated with different heavy liquid metals like Lithium-Lead alloy, Lead-Bismuth eutectic alloy and pure lead. LIFUS5/Mod3 (the third refurbishment) is a multi-purpose facility employed in fission and fusion technologies to address the issues related the HLM/water reaction interaction (Fig. 1). The test section S1A is devoted to the small leakage detection activity, objective of EC FP7 MAXSIMA Project. S1B is aimed at studying the interaction of PbLi and water in the framework of EUROfusion project.

2.1 Test matrix

The LIFUS5/Mod3 boundary conditions selected for the experimental campaign are consistent with the MYRRHA PHX design parameters.

A Test Matrix (TM) of 10 experiments were proposed. 50 laser micro-holed plates were constructed. The holes were from 5 to 200 µm. SEM analyses showed that the laser was not able to drill the stainless steel in the case 5 µm. No experiment was successful with the orifices having diameters 10 and 20 µm. These were plugged during the commissioning tests before the installation in LIFUS5/Mod3, notwithstanding the presence of a PORAL filter 0.5 µm, upstream the injector device. The remaining orifices dimensions were tested. It must be stressed that plugging was experienced during tests also in the cases 40, 60 and 80 µm.

Therefore, tests were performed adopting injection laser micro-holed plates having the diameters: 40, 60, 80, 100, 150 and 200 micrometers. The actual Test Matrix is reported in Tab. 1, while information about the properly work of data acquisition and leak detection system are reported in Tab. 2.

2.2 Objectives of the experimental campaign

The main objective is to investigate and correlate the size of a potential micro-crack presents on a tube of MYRRHA PHX tubes bundle with the noise that the vapor bubbles produce bubbling from it. In connection with this goal, the expected outcomes of the tests are:

- *the generation of reliable experimental data;*
- *the evaluation of the water mass flow rate in LBE through a characterized cracks;*
- *to correlate crack sizes with acoustic signals;*
- *the enlargement of database for code validation.*

Tab. 1 – LIFUS5/Mod3 experimental campaign – C series (from September 2017 to April 2018).

Parameter	TEST										
	C1.1 (_60)	**C1.2** (_60)	**C1.3** (_60)	**C2.1** (_80)	**C2.2** (_80)	**C3.1** (_40)	**C3.2** (_40)	**C4.1** (_100)	**C4.2** (_100)	**C5.1** (_150)	**C6.1** (_200)
Number of Test	T#1	T#7	T#10	T#2	T#9	T#3	T#6	T#4	T#5	T#8	T#11
Date of execution	06 Sep	19 Jan	8 Feb	13 Sep	2 Feb	20 Oct	15 Dec	10 Nov	22 Nov	26 Jan	6 Apr
Number of laser-holed plate [3]	21	22	23	16	19	27	28	11	13	6	4
Injector orifice design diameter [µm]	60	60	60	80	80	40	40	100	100	150	200
Injector orifice measured flow area [μm^2]	3188	3080	3257	4919	5508	1392	1329	8116	7676	18768	32151
Execution	ok	failed	ok	ok	ok	failed	ok	failed	ok	ok	ok
Acquisition time [hh:mm]	06:15	NA	09:00	11:22	5:00	NA	5:29	NA	7:29	5:59	3:00
LBE temperature TC-S4A-01 [°C](1)	203	NA	226	209	226	NA	NI	NA	NI	226	246
Water pressure PC-S2V-01 [bar](1)	19.7	NA	20.1	20.2	19.3	NA	NI	NA	NI	20.3	20.2
Water temperature TC-S2L-08 [°C](1)	170	NA	219	200	210	NA	NI	NA	NI	203	247

(1) Pressure and Temperature identified at SoT

Tab. 2 – LIFUS5/Mod3 experimental camping – Synoptic and leak detection system acquisition.

# TEST	Synoptic	ADS1	ADS2	ADS3	ADS4	ADS5	HTA	HSA	AE
C1.1_60	Ok	yes	no	yes	no	no	yes	yes	yes
C1.3_60	Ok	yes	no	no	no	no	yes	yes	yes
C2.1_80	Ok	no	yes	no	no	no	yes	yes	yes
C2.2_80	Ok	no	no	no	no	no	yes	yes	yes
C3.2_40	Failed	no	yes	yes	no	no	--	--	--
C4.2_100	Failed	yes	yes	yes	no	no	--	--	--
C5.1_150	Ok	yes	no	no	no	no	yes	yes	yes
C6.1_200	Ok	yes	no	no	no	no	yes	yes	yes

2.3 Facility description

LIFUS5/Mod3 is the upgrade of the previous configuration of LIFUS5/Mod2 (Refs. [4]-[6]). The facility can be operated at maximum temperature of 500 °C and maximum pressure of 200 bar, according to PED directive. It is composed by four main components:

- the interaction vessel S1A, where LBE/water interaction occurs;
- S2V vessel, where demineralized water is stored for the injection in S1A by means of a pressurized gas cylinder connected to the top;
- S4A is the storage tank of LBE;
- S3V is a dump tank, used to collect vapor and gases during the test.

The main parts characterizing LIFUS5/Mod3 facility are shown in Fig. 2.

The interaction vessel S1A is about 100 liters, and it is partially filled with LBE during the tests. A top flange closes it by means of a gasket spiral wound graphite filled. Considering LIFUS5/Mod3, the compression force is given by 20 bolts that are subjected to a tightening torque of about 250 Nm. Penetrations are made in S1A top flange (Fig. 3) for allowing the installation of the instrumentation and connections:

- ½" sch. 40 penetrations for two on/off level meters (LVs);
- 1" sch. 40 penetrations for five Acoustic Detection (ADS) systems;
- ½" BWG penetration for one absolute pressure transducer (PC) and for S1A atmosphere inerting by means of a T connection;
- 1" sch. 40 penetrations for a very high temperature accelerometer (HTA);
- 1" sch. 40 penetrations for a low temperature high sensitivity accelerometer (HSA);
- 1" sch. 40 penetrations for an Acoustic Emission (AE) detection system;
- 3" sch. 80 pipe connection to S3V dump tank.

Internally, S1A can be divided into an upper cylindrical part and a lower hemispherical part. The main diameter is 420 mm and the overall height is 780 mm. The cylindrical shell of S1A has penetrations allowing the passage of the instrumentation. These consist of:

- one fast pressure transducers (PT),
- two thermocouples (TCs);
- six strain gages (SGs), five of which set on the inner S1A surface and one on the outside.

At the bottom of the vessel, a 2" sch.80 penetration provides the connection with the injection line and the LBE charging/discharging system (Fig. 4).

The water tank S2V (Fig. 5 and Fig. 6) is a pipe, closed at the edges with two flanges. It has a volume of about 14 liters. It is connected on the top with the gas line, which is used for setting and keeping the pressure of the water according with the test specifications. On S2V top flange, a threaded penetration is provided allowing the passage of a magnetostrictive level measurement device (which has the sensitivity of 5 mm, and shown in Fig. 7), having a volume of 3 liters. The filling level in the S2V vessel is continuously monitored also by a DP meter inserted between the lower part of S2V and bottom part of injection line, for an high of about 2.15 m.

At bottom, S2V is connected with a ¼" sch. 80 pipe to the water injection line. Further penetrations, in the upper part of S2V, consist in:

- one absolute pressure transducer (PC);
- two thermocouples (TCs);
- three ¼″ sch. 80 pipes:
  - to connect a safety valve (VS-S2V-01);
  - to connect input (by valve VE-S2V-02) and output (by valve VE-S2V-03) gas line;
  - to connect water charging (by valve VE-S2V-06).

LBE in S1A is filled and drained, just before and after the test respectively. It is stored in the **liquid metal storage tank S4A** (Fig. 8), which is connected to the bottom of the main vessel S1A. On lateral surface of S4A penetrations are provided allowing the passage of instrumentation:

- one absolute pressure transducer (PC);
- one thermocouple (TC);
- two on/off and one continuous level meters (LV).

Further penetrations, consist in:

- three ½ " BWG:
- two to connect input (by valve VE-S4A-01) and output (by valve VE-S4A-04) gas line;
- one to purifies LBE (this line has to penetrate S4A up to 3-5 cm from the bottom);
- one 1" sch. 40 to connect the safety valve VS-S4A-01;
- one 1" sch. 40 ANSI 300 to carry out the first LBE charge and the charging/discharging with S1A.

The dump tank S3V (Fig. 9) is part of previous LIFUS5/Mod2 facility (Ref. [6]). It is connected by means of a 3" line to the top flange of S1A. The S3V volume is equal to 2 m^3 and the design pressure is 1 MPa. It represents a safety volume used to collect the vapour and the gas generated by the interaction between LBE and water.

LIFUS5/Mod3 DACS (Data Acquisition and Control System) is realized using National Instruments hardware and software.

A mix of Compact Field Point and Compact RIO modules are used as hardware. LIFUS5/Mod3 DACS architecture is logically divided in two separate sections: real time control and data acquisition (CTRL) and control, interlock and safety system (CISS). CISS is a separate subsystem dedicated to the protection of the operators and of the plant. CTRL is divided into the Human Machine Interface (HMI) and Supervisory Control And Data Acquisition (SCADA). The HMI (Human Machine Interface) and SCADA (Supervisory Control And Data Acquisition) run on standard x86 PC/Workstation and it is developed using LabVIEW software. All components will be connected using standard Ethernet. The LIFUS5/Mod3 synoptic is shown in Fig. 2.

Exception is the acquisition of the ADS microphones, accelerometers and acoustic emission sensors, which have dedicated hardware and software.

The ADS system is dedicated to acquire the sound pressure wave generate from the water injection into PbLi. It is composed of: a standard PC with gnu/linux OS, an external multichannel ADC card and 5 microphones. The PC is connected to the external ADC by a proprietary bus 10 meter long. The PC is placed inside the electrical cabinet, the ADC near the test tank and the microphones are placed radially inside the cover of S1A. The aim of the system is to record the sound pressure wave of the water injection inside the PbLi and convert it to an electrical signal in order to evaluate the sound pressure wave generated from different orifice diameters.

2.4 Injection line

Injection line starts from S2V water storage tank and it is connected to the S1A reaction vessel. A Coriolis mass flow meter (MT-S2L-01) is placed between the pneumatic valves VP-S2L-07 and VP-S2L-08, in order to measure the mass of water that flows in the line and is injected in reaction tank S1A. A manual drainage valve (VM-S2L-11) is located downstream the mass flow meter, with the aim to empty the line after every experimental procedure. The Coriolis has the capability to measure the mass flow rate in the range of 50 - 2000 g/h.

The water injection line is heated from VP-S2L-08 (downstream the Coriolis) to S1A. There are 5 heating wires in charge to warm-up the water before its entering in the reaction vessel (up to 200°C). These heating wires are controlled by means of thermocouples, both safety and regulation. The temperature of the fluid is regulated with 4 thermowells. Line is insulated from the external environment by an insulating layer, this reduces the heat losses and therefore limits the power of heating wires. Fig. 10 and Fig. 11 show the water injection line.

2.5 Injection system

The injection system (Fig. 12) is constituted by two separate parts, connected by a 2”ANSI 2500 RJ flange. The first one is completely integrated and welded to the bottom of S1A vessel. The second one is manufactured by four coaxial tubes and it can be dissembled at the end of each test to allow the replacement of the injector device.

The 1/8” BWG water injection line enters into a second tube of ½” BWG. The second tube permits the inlet of the gas for the injection system cooling. The gas flows towards up to the injector device and then flows in counter-current direction into the 1” BWG third tube, designed for the gas outlet. The LBE is charged and discharged through the fourth tube of 2” sch. 80.

2.6 Injector device

The injector device (Fig. 13) is characterized by a micro-holed AISI 316 plate with a thickness of 1 mm and a diameter of 1” (25.4 mm). At the center of the plate, a single micro-hole is manufactured by laser technology. The specifications of the 45 laser micro-holed plates are reported in [3] and it varied from 5 to 200 μm. The injector penetrates into S1A interaction tank of 170 mm.

The plate is installed into the injector device between two graphite sealing rings. An injector cap closes the injector device by means of a spanner, designed ad hoc. In this way, at each test, the injector device can be disassemble and the plate can be replaced with another one with different micro-hole diameter. All of these components are manufactured by ENEA workshop.

2.7 Installed Components

The main components installed on the facility, as reported in the synoptic (Fig. 2) are listed in the following tables (Tab. 5 and Tab. 6).

2.8 Detection System: Real Time Data Acquisition For Acoustic Sensors

This section describes the hardware structure used to acquire the sound signal coming from the microphone placed on the flange of the LIFUS5/Mod3 facility.

The top flange of the facility has 5 penetrations where the microphones are installed (ADS). These are:

- PCB PIEZOTRONICS Model 130E20 (quantity 4);
- PCB PIEZOTRONICS Model 377B26 (quantity 1), central position.

The layout is depicted in Fig. 14.

2.8.1 PCB 130E20

The PCB Model 130E20 (Fig. 15) are pre-polarized microphones, condenser microphones coupled with ICP sensor powered preamplifiers and are thus referred to as ICP microphones (an integrated circuit piezoelectric sensor or ICP sensor is a device used to measure dynamic pressure, force, strain, or acceleration). These Microphones are 7 mm in diameter and have a dynamic range up to 122 dB. The maximum temperature for this kind of microphone is 50°C.

The microphone is provided of a BNC connector useful for the faster connection of the pre-amplifier. The preamplifier could be manually regulated to adapt the output signal to the input range of the ADC system (gain x1, x10, x100).

2.8.2 PCB 377B26

The PCB Model 377B26 Probe Microphone (Fig. 16) is a compact unit for sound pressure measurement in small enclosures, harsh environments, and close proximity to sound sources. The high acoustic input impedance of the probe tip minimizes the influence on the acoustic field, while the 160 mm stainless steel probe tube can withstand temperatures of up to 800 ºC. The Probe Microphone is internally compensated to equalize the static pressure at the probe tip with the internal microphone pressure. The probe is constructed with a detachable stainless steel probe tip, which guides the acoustical signal to a microphone inside the probe housing. The probe can be used with both stainless steel probe tips and flexible tube tips of different lengths. After being measured, the acoustical pressure wave is passed on to an impedance-matched wave guide, which eliminates internal reflections. This results in a smooth frequency response from 2 Hz to 20 kHz. The internal microphone is connected to a low noise preamplifier with high dynamic range.

2.8.3 Acquisition system hardware

For the Analogic to Digital conversion will be used a PCI card with specifications:

- Resolution: 16 bit
- Number of channel: 8;
- Sampling rate > 150kS/s;
- Programmable gains;
- OS driver: comedi.

The board is National Instruments PCI-6221. This is installed inside a PC placed on the electrical cabinet of LIFUS5/Mod3 facility.

The software is

- OS – GNU/Linux Debian 8.0;
  - RT_PREEMPT real time patch for linux;
  - Comedilib: a user-space library that provides a developer-friendly interface to Comedi devices.
  - Comedi driver: a collection of drivers for a variety of common data acquisition plug-in boards. The drivers are implemented as a core Linux kernel module providing common functionality and individual low-level driver modules.

The software is developed in C and C++ language. The interface between the ADC card is given by the ADC-driver. The signal is analyzed in:

- time domain;
- sound pressure;
- sound intensity;
- sound power;
- frequency response.

The sampling rate is fixed to 20 kHz.

- Cooling system

The maximum temperatures for the microphones are:

- 50 °C for the four external microphones (PCB 130E20);
- 650°C for the central microphone (PCB 377B26).

A cooling system has been studied to avoid damage to the microphones PCB 130E20 due to the high temperature of the LBE and of the top flange. It is composed of 3 parts:

1. Metallic support: this prevents the leakage of gas and leaves the space to the microphone to measure the sound coming from the liquid.
2. Ceramic support: this grants the thermal insulation between the cover/metallic support and the microphones;
3. Cooling gas: in charge of keeping the low temperature microphones (PCB 130E20) at a temperature below the design values. The cooling system layout is reported in Fig. 17.

The cooling system is based on a pipe 1” BWG, a ceramic support, and Ar gas flowing through a 1/8” tubing. The ceramic support (Fig. 18) has been fabricated to keep the microphone to the position allowing the Ar gas cooling. The characteristics are:

- Central hole dimensioned to place the microphones;
- Two lateral channels (radially placed) used to flux the Argon to the tip of the microphone.

The overall assembly is depicted in Fig. 19.

2.9 Detection System: Accelerometers And Acoustic Emission Sensor

This section describes the hardware structure used to acquire the sound signal coming from an alternative detection system, which is constituted by accelerometers and acoustic emission sensor placed on the flange and inside the vessel of the LIFUS5/Mod3 facility. The layouts are depicted in Fig. 21, Fig. 22, and in Fig. 23.

The top flange of the facility has other 3 penetrations where the sensors are installed, see Fig. 20. These alternative detection systems are:

I. Inductive proximity sensor (i.e. High Sensitivity Accelerometer – HSA) installed outside the vessel;
II. Accelerometer sensors installed inside the vessel (i.e. High Temperature Accelerometer – HTA) on a metallic support;
III. Acoustic Emission (AE) sensor installed outside the vessel, measuring the high frequency signals by means of a waveguide.

2.9.1 Wilcoxon Research model 786-500

The High Sensitivity Accelerometer (HSA) is a inductive proximity and a low frequency sensor with a ±5% sensitivity tolerance. It is installed on the top flange of S1_A interaction vessel as reported in Fig. 21.

The main features of the sensor are:

- Rugged design;
- High sensitivity;
- Hermetic seal;
- ESD and reverse wiring protection;
- Clear signals at low vibration levels;
- Extended low end frequency response;
- Improved signal to noise ratio versus other general purpose accelerometers;
- Detection of both low and high speed vibrations.

2.9.2 IMI Sensor Series EX600B13

The High Temperature Accelerometer (HTA) is installed inside the vessel S1_A by means of a supporting structure of AISI316L, designed and manufactured in ENEA Workshop. The layout of installation is reported in Fig. 22. The main features of the sensor are:

- Sensitivity of ±5% of 100 mV/g (10 mV/g),
- Withstands temperature up to 482 °C,
- UHT-12 sensing element;
- Inconel housing material,
- Hermetic welded sealing,

2.9.3 HOLROYD Instruments 24/7 Ultraspan

The Acoustic Emission (AE) sensor is installed outside the vessel, measuring the high frequency signals by means of a waveguide (Fig. 23). The active face (base) of the 24/7 Ultraspan sensor detects the high frequency component of naturally occurring structure borne stress waves (known as Acoustic Emission or AE). To do this, the base of the sensor must be acoustically coupled to the surface of the item of interest using a suitable coupling material. In this case, the use of a waveguide is necessary to interface the base of the sensor with the material being monitored (the LBE and the water bubbles due to the micro-crack inside). The AISI316L waveguide is designed and manufactured by ENEA Workshop.

2.9.4 Multichannel acquisition system

In order to acquire and process the experimental data of the accelerometers and acoustic emission sensor, it was necessary to assembly a specific electric cabinet, containing the multichannel DAWESOFT - SIRIUS® system (Fig. 24). The data are acquired and processed by means of its proprietary software.
The accelerometers and the acoustic emission sensor, described in the previous sections, are connected to the multichannel acquisition system, which produces electrical signals at high frequency.

The multichannel amplifies, converts and sends the signals to the acquisition system run on industrial PC. By means of the proprietary software (Fig. 25), the data are saved as pure signals of sensors, and as elaborated data such as FFT, RMS or peak signals in binary proprietary format. The software permits also to export data in other format suitable to be processed with other programs.

Tab. 3 – LIFUS5/Mod3: tanks features.

COMPONENT	Parameter	Value
S1A	Volume [m^3]	0.1
	Inner diameter [m]	0.42
	Height [m]	1.085
	Design pressure [bar]	200
	Design temperature [°C]	500
	Material	AISI 316
S2V	Volume [m^3]	0.015
	Inner diameter	4 inch sch. 160
	Design pressure [bar]	200
	Design temperature [°C]	350
	Material	AISI 316
S3V	Volume [m^3]	2.0
	Inner diameter [m]	1
	Design pressure [bar]	10
	Design temperature [°C]	400
	Material	AISI 316
S4A	Volume [m^3]	0.42
	Inner diameter [m]	0.544
	Design pressure [bar]	10
	Design temperature [°C]	450
	Material	AISI 316

Tab. 4 – LIFUS5/Mod3: S1A flange penetrations.

POS.	NO.	DN	UTILIZATION
A	1	3''	S1-S3 connection
B	1	1''	Microphone 1
C	1	1''	Microphone 2
D	1	1''	Microphone 3
E	1	1''	Microphone 4
F	1	1''	Microphone 5
G	1	½ ''	ON/OFF level meter
H	1	½ ''	ON/OFF level meter
I	1	½ BWG	Absolute pressure transducer (PC-S1A-01) and gas inerting
L	1	1''	AE acoustic emission sensor
M	1	1''	HSA accelerometer
N	1	1''	HTA accelerometer

Tab. 5 – Valves/Pressure reducers list.

#	ID	Location		Type	Notes
		SYS	Zone		
1	RP-S4A-01	S4A	Tank	Pressure regulator	Manual
2	RP-S4A-02	S4A	Tank	Pressure regulator	Manual
3	RP-S2V-01	S2V	Tank	Pressure regulator	Manual
4	RP-ADS-01	ADS	Line	Pressure regulator	Manual
5	VE-S4A-01	S4A	Tank	Electro Valve	Electrical
6	VE-S4A-02	S4A	Tank	Electro Valve	Electrical
7	VE-S4A-03	S4A	Tank	Electro Valve	Electrical
8	VE-S4A-04	S4A	Tank	Electro Valve	Electrical
9	VS-S4A-01	S4A	Tank	Safety valve	Passive
10	VM-S4A-01	S4A	Tank	Manual valve	Manual
11	VP-S4A-01	S4A	Line	Pneumatic valve	Pneumatic
12	VP-S2L-08	S2L	Line	Pneumatic valve	Pneumatic
13	VP-S2L-09	S2L	Line	Pneumatic valve	Pneumatic
14	VM-S2L-11	S2L	Line	Manual valve	Passive
15	VP-S2L-07	S2L	Line	Pneumatic valve	Pneumatic
16	VE-S2V-05	S2V	Line	Electro Valve	Electrical
17	VN-S2V-01	S2V	Line	Non-return valve	Passive
18	VE-S2V-02	S2V	Line	Electro Valve	Electrical
19	VE-S2V-06	S2V	Line	Electro Valve	Electrical
20	VE-S2V-03	S2V	Line	Electro Valve	Electrical
21	VS-S2V-01	S2V	Tank	Safety valve	Passive
22	VP-S3V-02	S3V	Line	Pneumatic valve	Pneumatic
23	VE-S3V-01	S3V	Tank	Electro Valve	Electrical
24	VE-S3V-02	S3V	Tank	Electro Valve	Electrical
25	VE-S1A-01	S1A	Line	Electro Valve	Electrical

Tab. 6 – Installed heating wires.

#	ID	Location		Type	Power [kW]
		SYS	Zone		
1	CS-S4A-1A	S4A	S4_A storage tank	Heating wire	2.07
2	CS-S4A-1B	S4A	S4_A storage tank	Heating wire	0.99
3	CS-S4A-1C	S4A	S4_A storage tank	Heating wire	1.96
4	FS-S4A-04	S4A	Flexi Pipe	Heating tape	0.54
5	CS-S4A-02	S4A	Fill and Drain Line	Heating wire	1.54
6	CS-S4A-03	S4A	Fill and Drain Line	Heating wire	1.02
7	CS-S2L-06	S2L	Helical Water Line	Heating wire	1.49
8	CS-S2L-05	S2L	Helical Water Line	Heating wire	1.56
9	CS-S2L-04	S2L	Helical Water Line	Heating wire	1.51
10	CS-S2L-03	S2L	Water Line	Heating wire	2.50
11	FS-S2L-07	S2L	Water Line	Heating tape	0.54
12	CS-S1A-06	S1A	Injector device	Heating wire	0.95
13	CS-S1A-05	S1A	S1A reaction tank	Heating wire	1.50
14	CS-S1A-01	S1A	S1A reaction tank	Heating wire	2.50
15	CS-S1A-02	S1A	S1A reaction tank	Heating wire	2.50
16	CS-S1A-03	S1A	S1A reaction tank	Heating wire	3.50
17	CS-S1A-04	S1A	S1A reaction tank	Heating wire	3.00
18	CS-S3V-01	S3V	S3 dump tank	Heating wire	5.00
19	CS-S3V-02	S3V	S3 dump line	Heating wire	1.00
20	CS-S3V-03	S3V	S3 dump line	Heating wire	3.00
21	CS-S3V-04	S3V	S3 drain line	Heating wire	0.76
22	CS-S2V-01	S2V	S2 water tank	Heating wire	3.50
23	CS-S2V-02	S2V	S2 water tank	Heating wire	3.50

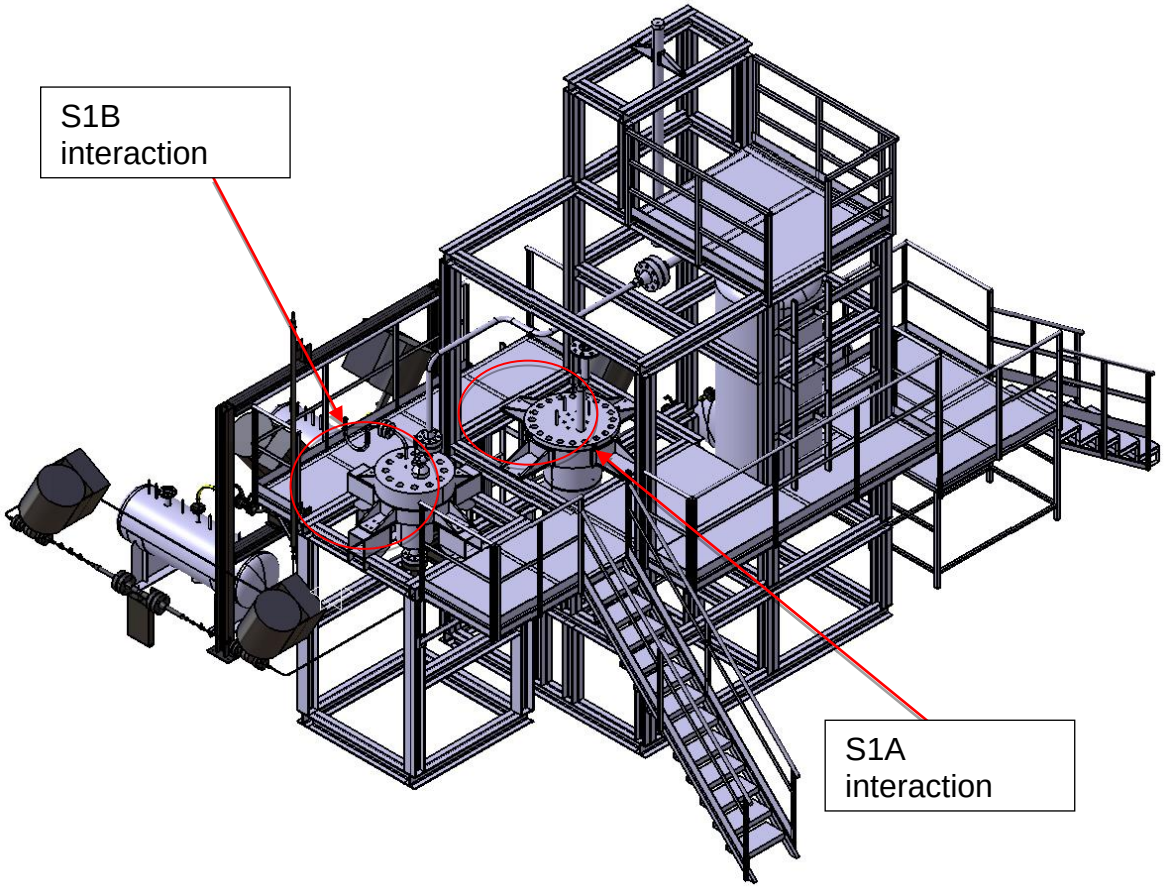

Fig. 1 - 3D drawing of LIFUS5/Mod3 with S1B and S1A identification.

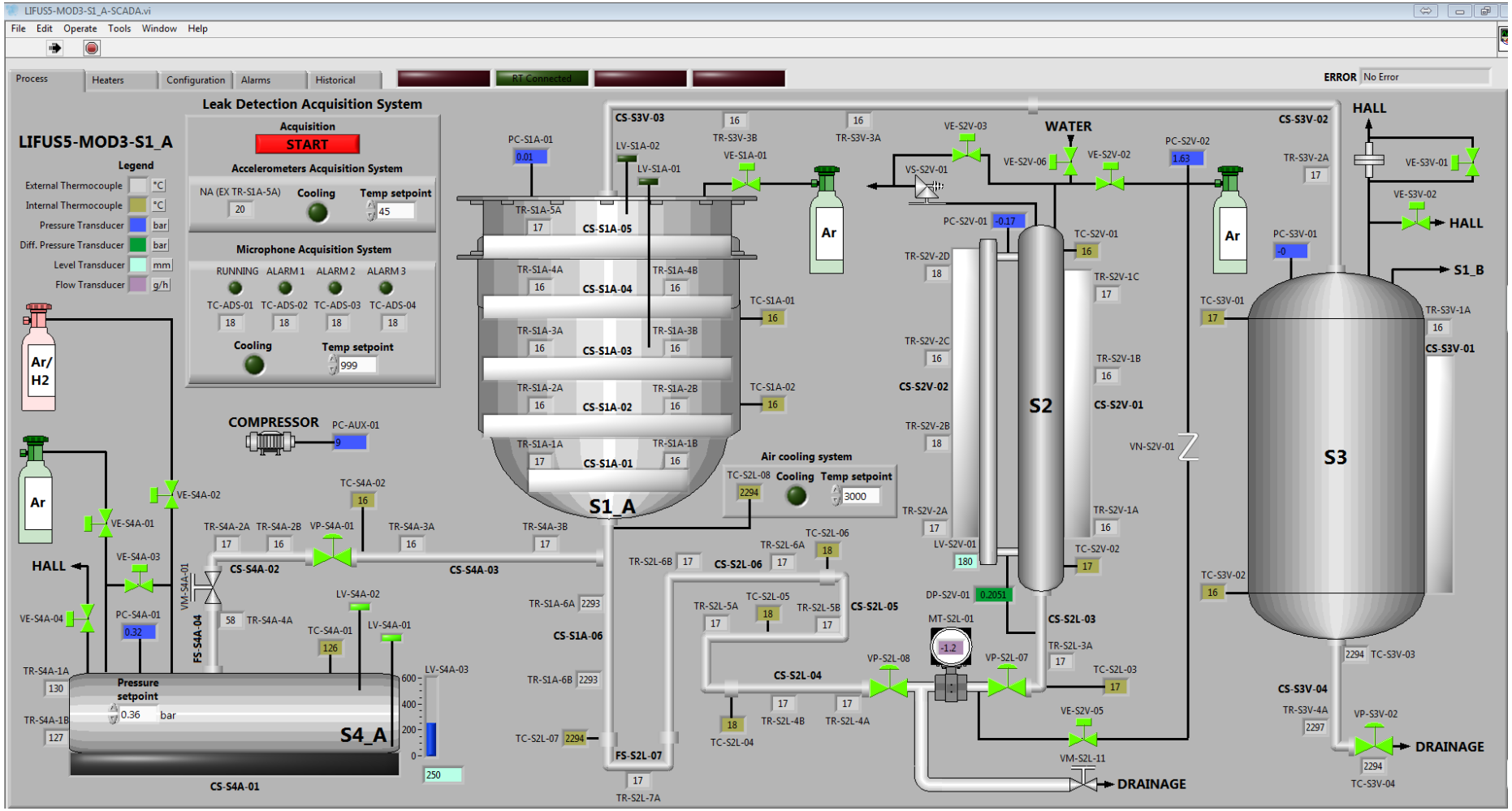

Fig. 2 – LIFUS5/Mod3 synoptic.

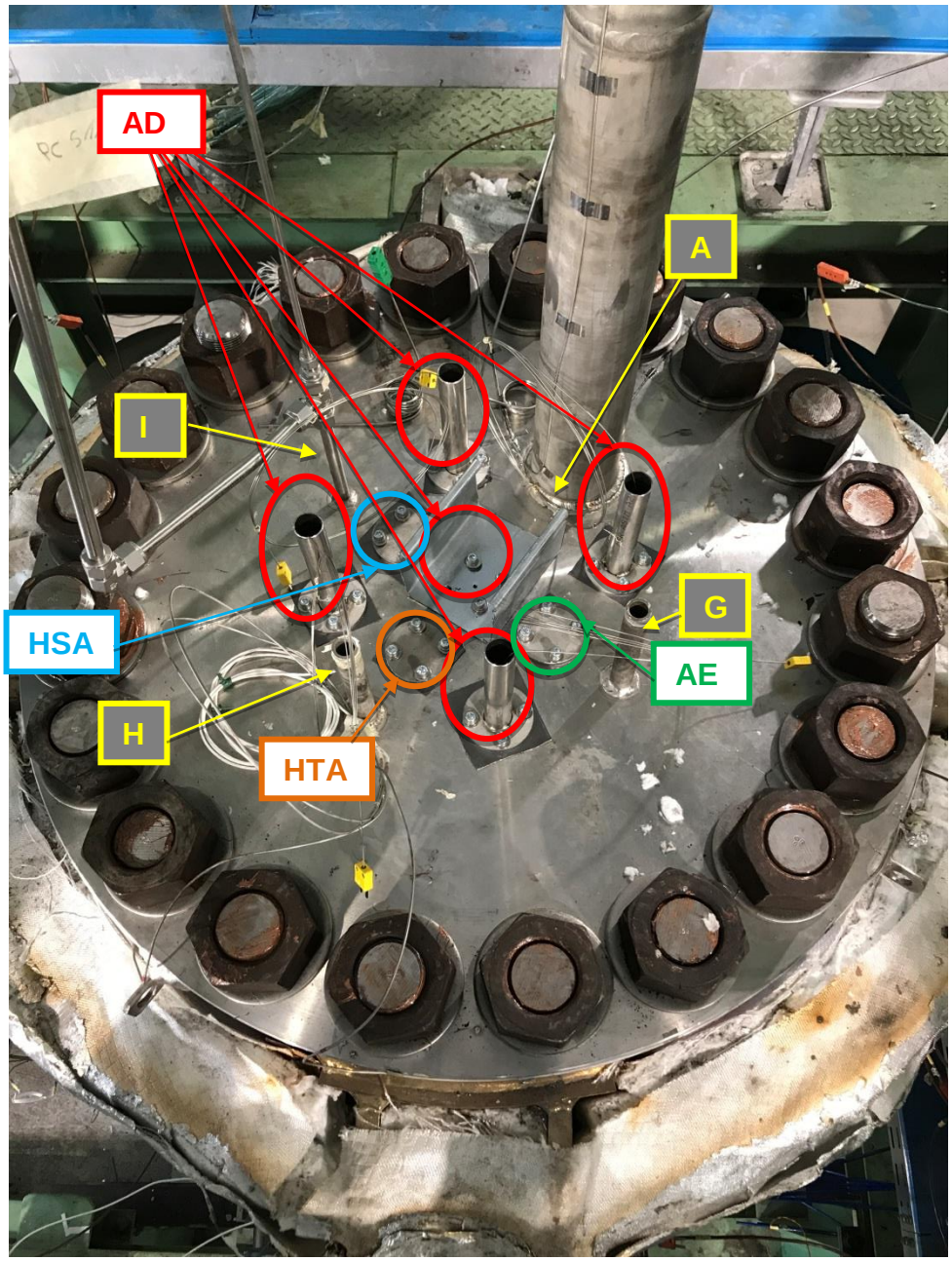

Fig. 3 – View of S1A flange penetrations

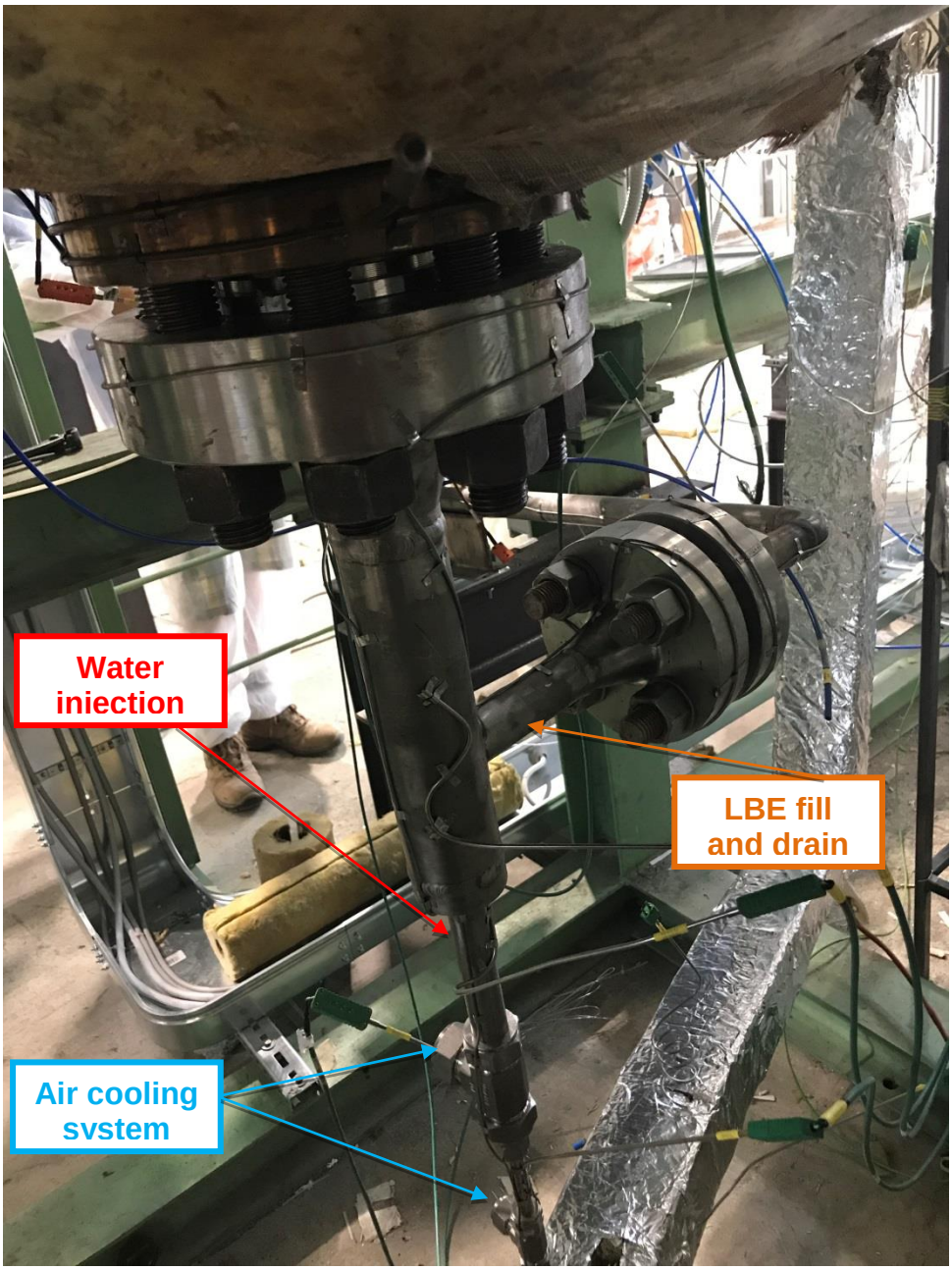

Fig. 4– S1A bottom flange and injection system.

Fig. 5 – S2V and level measurement systems.

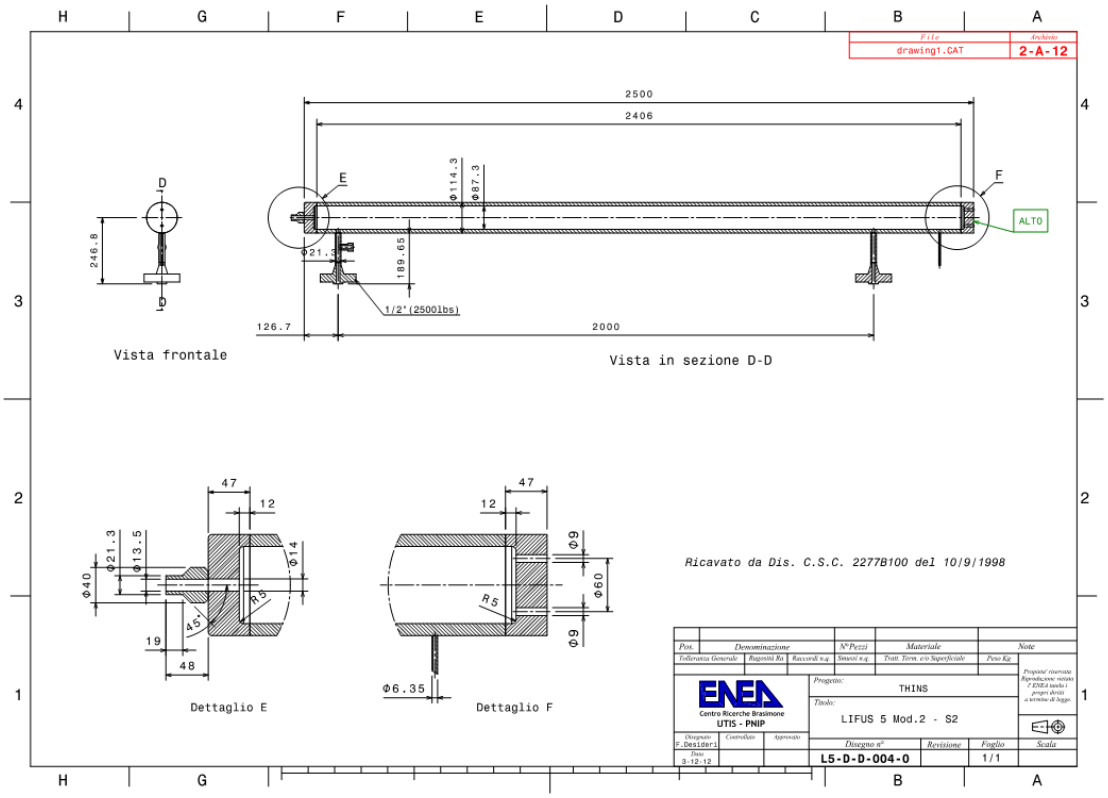

Fig. 6 – S2V system geometry.

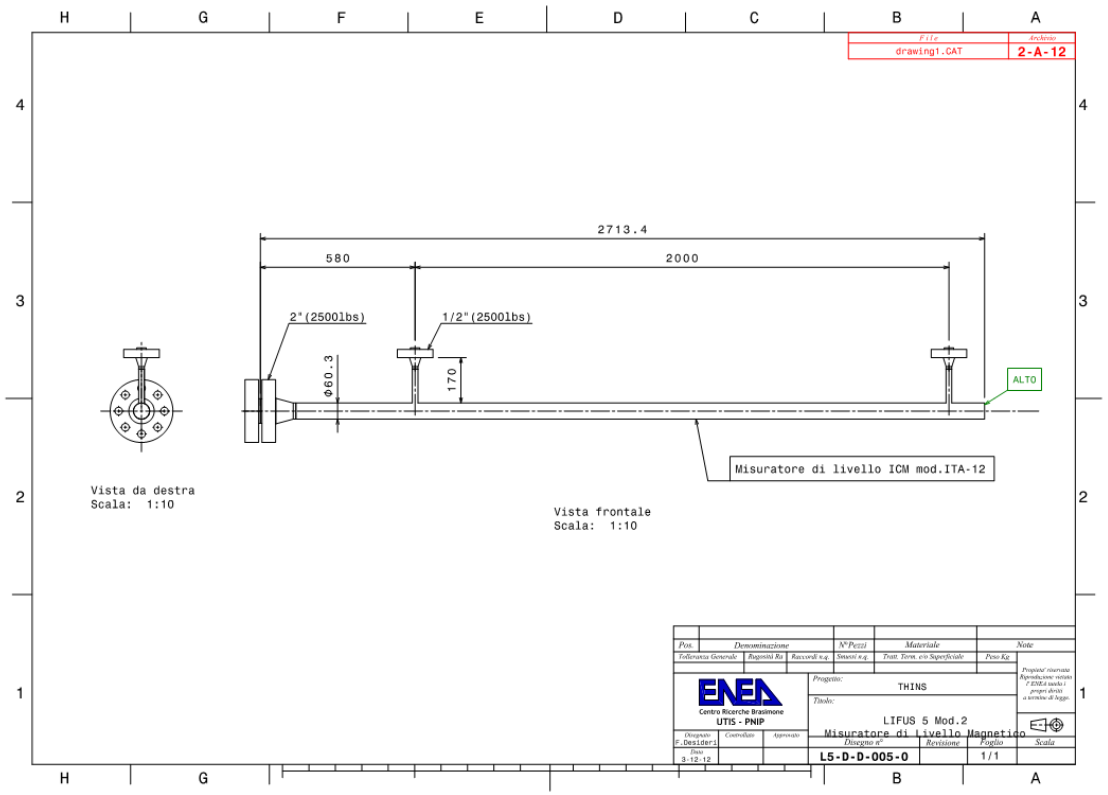

Fig. 7 – Level measurement system geometry.

Fig. 8 – S4A storage tank.

Fig. 9 – S3V dump tank.

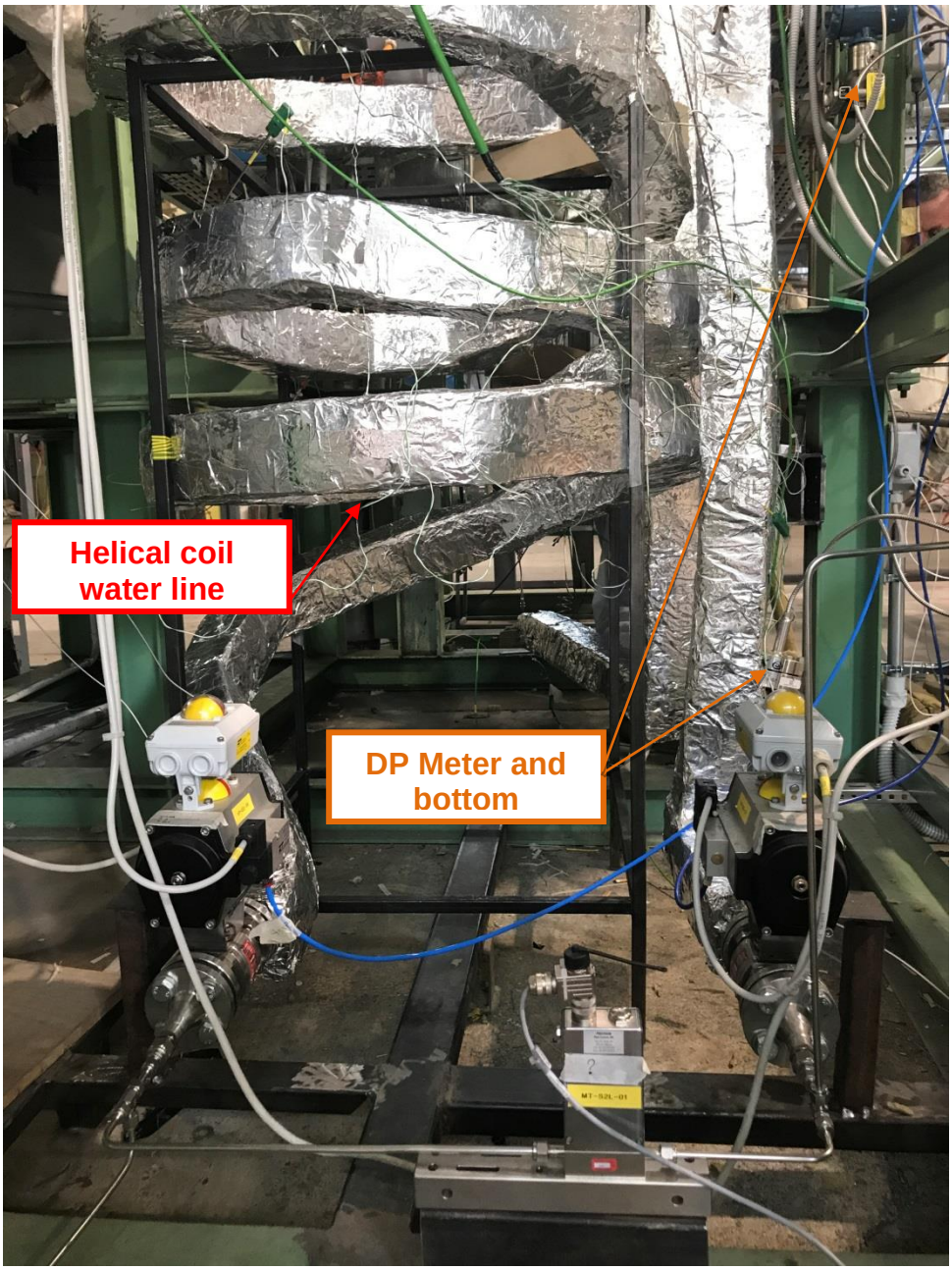

Fig. 10 – Water injection line.

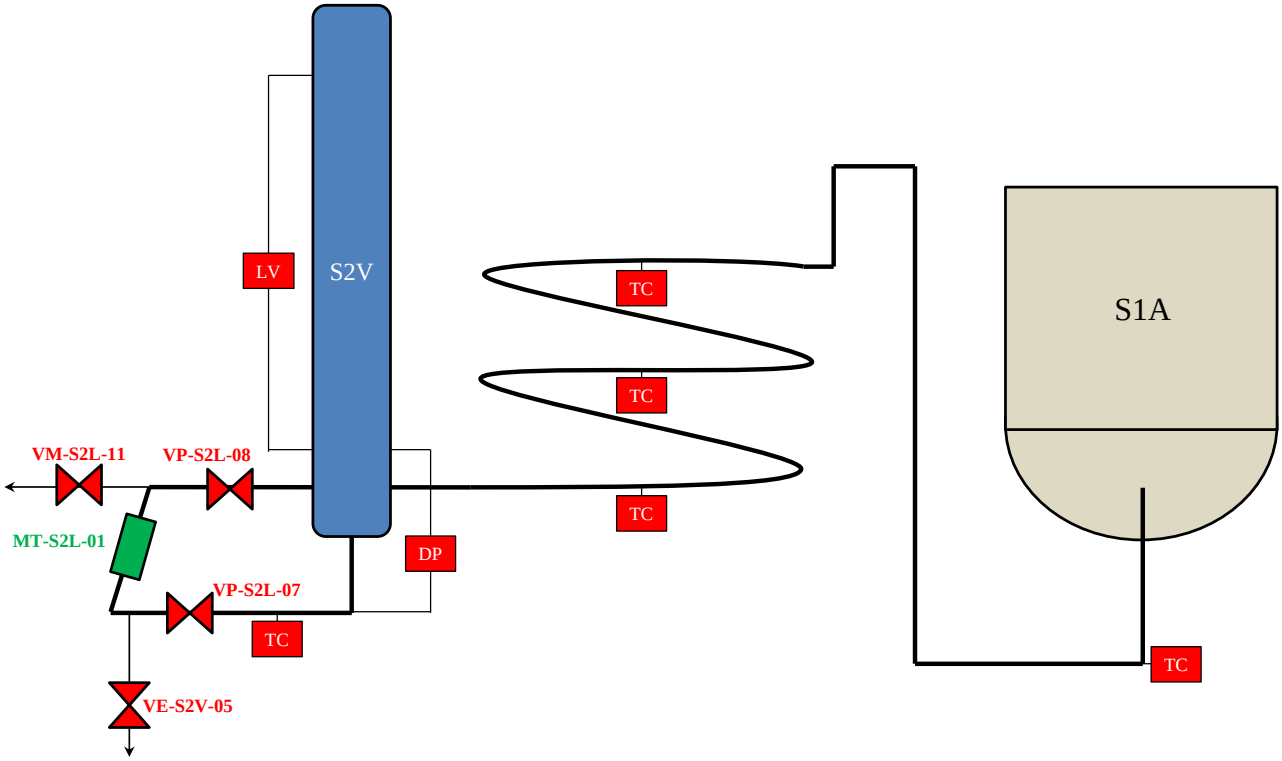

Fig. 11 – Sketch of water injection line.

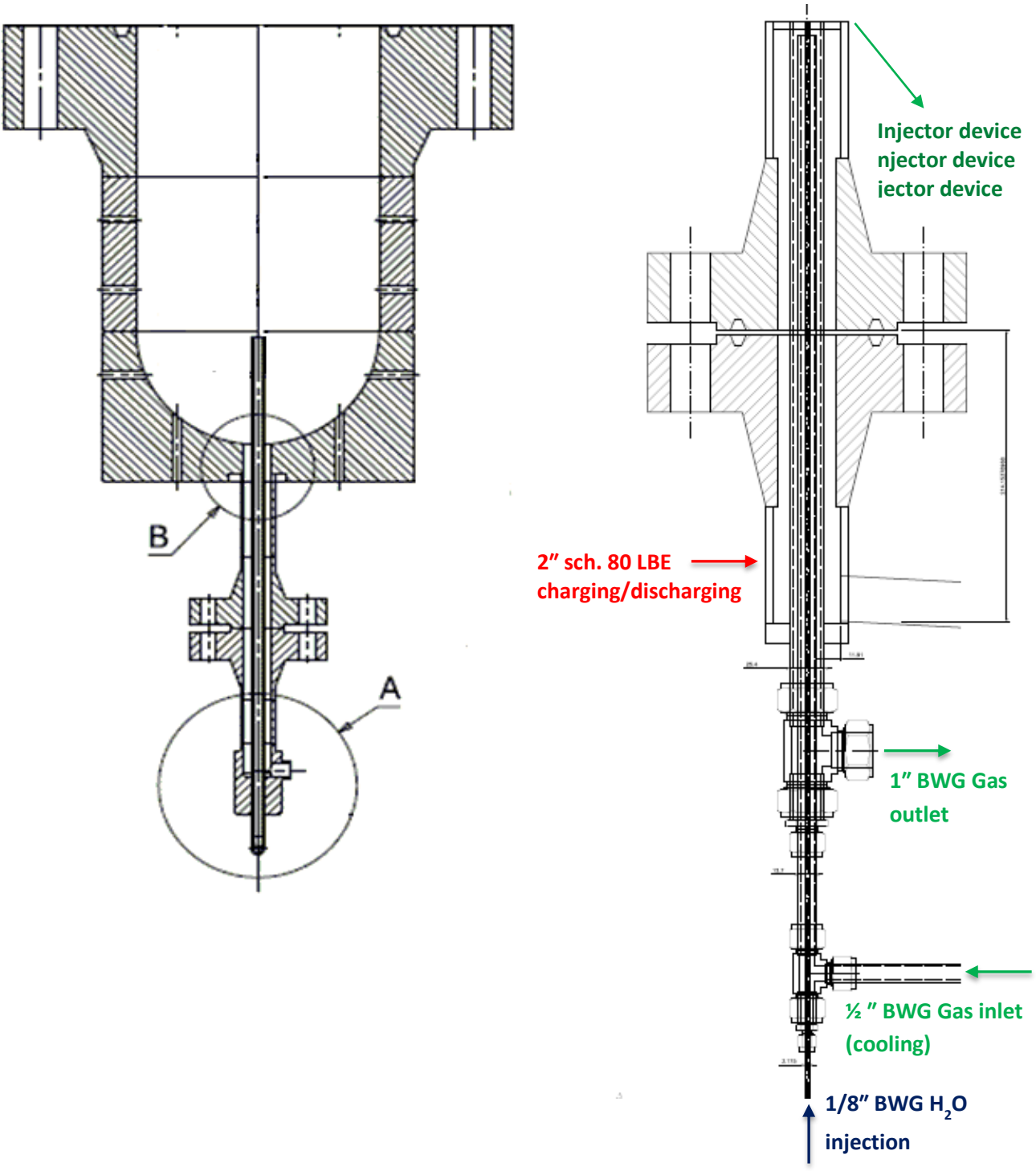

Fig. 12 – Sketch of the injection system and main dimensions.

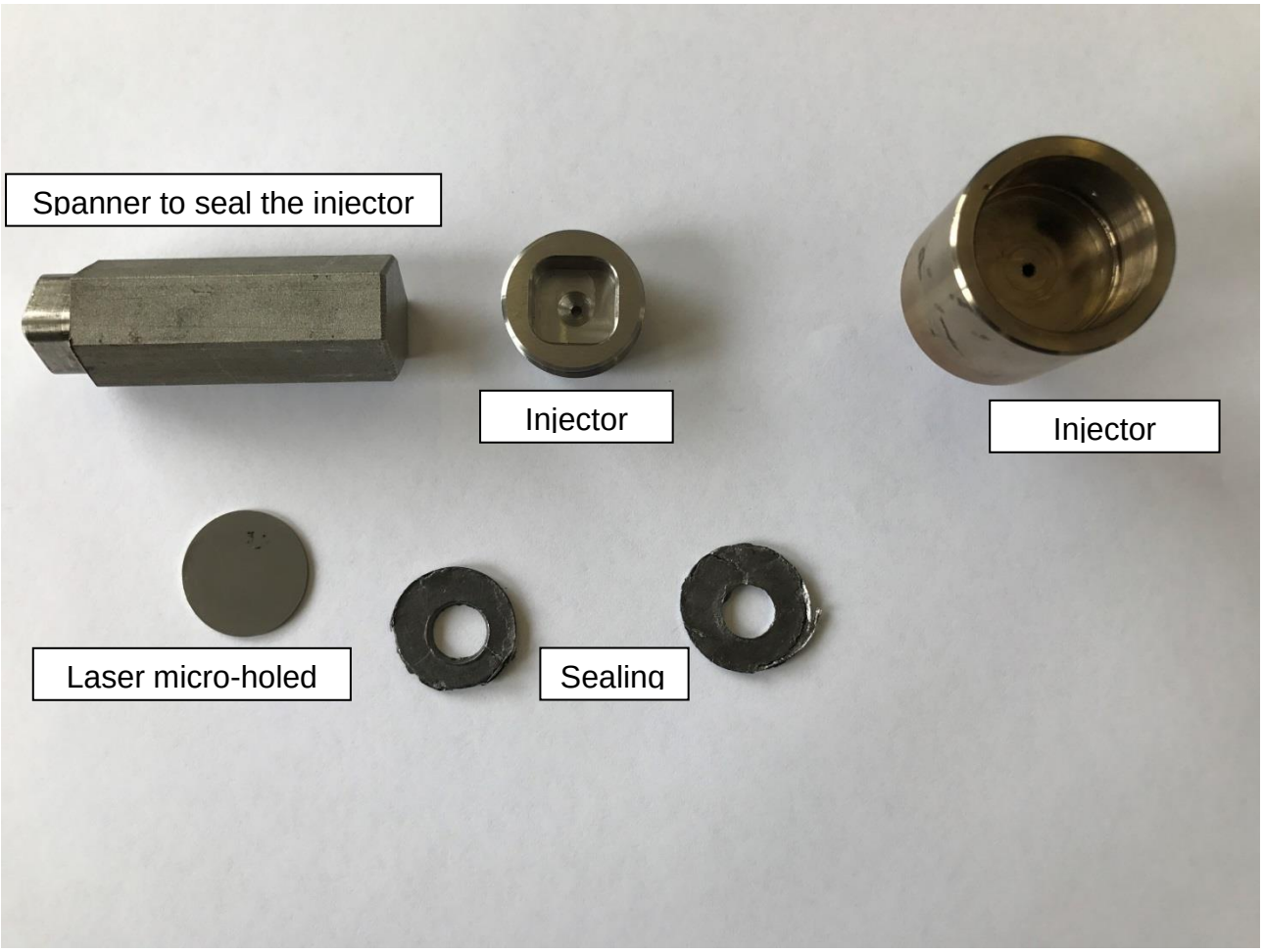

Fig. 13 – Injector system device.

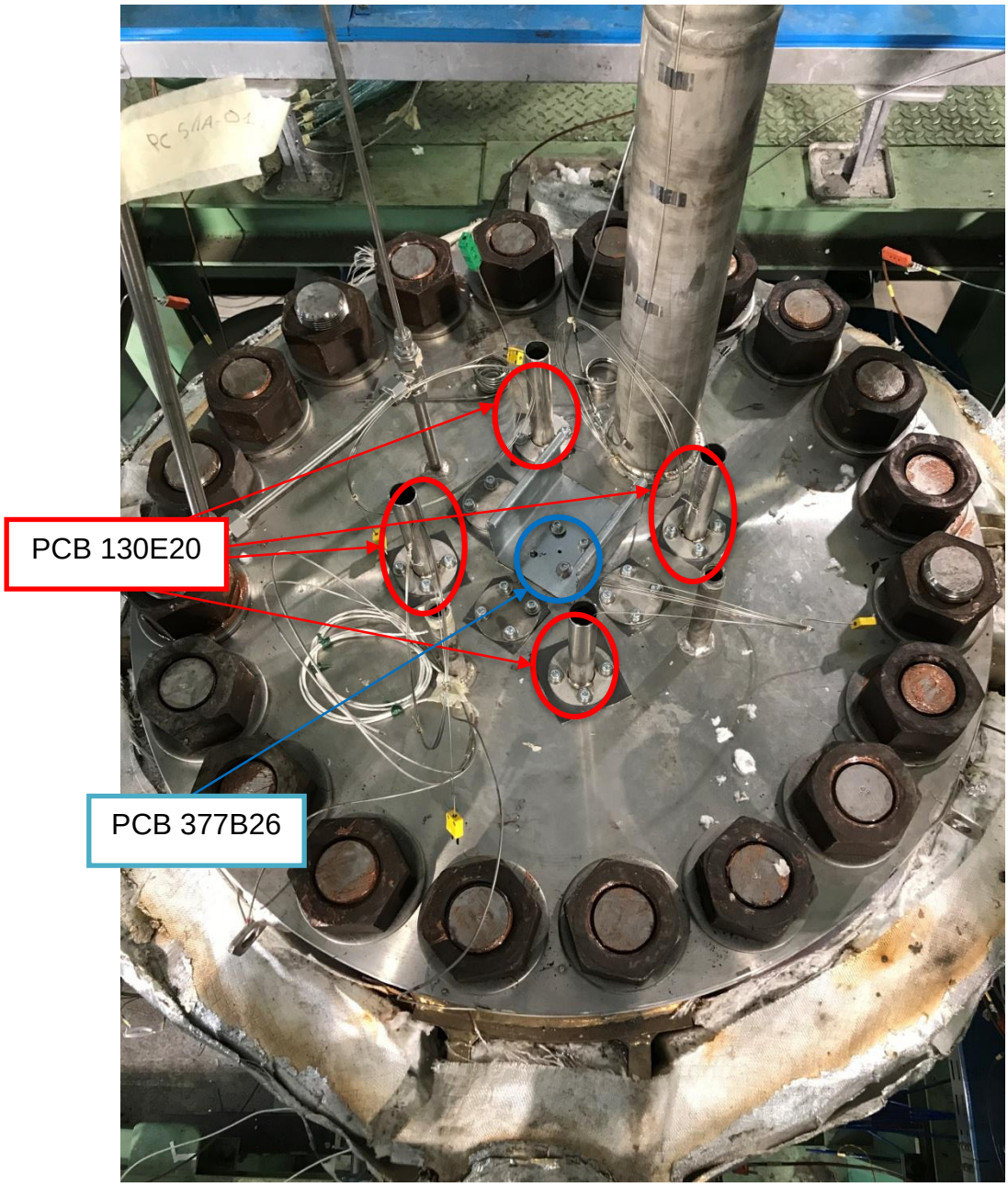

Fig. 14 – Microphones layout on the top flange of LIFUS5/Mod3 facility.

Fig. 15 – PCB 130E20 microphone.

Fig. 16 – PCB 377B26 microphone.

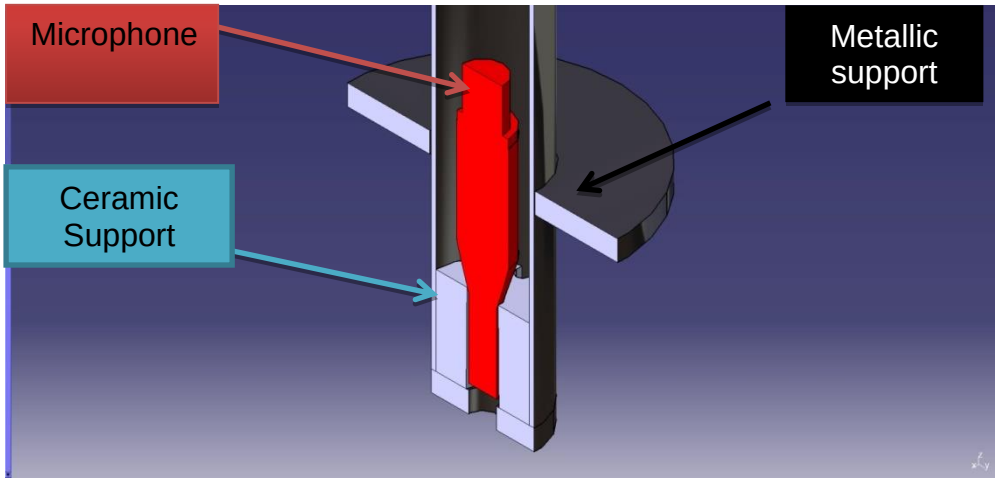

Fig. 17 – Cooling system assembly.

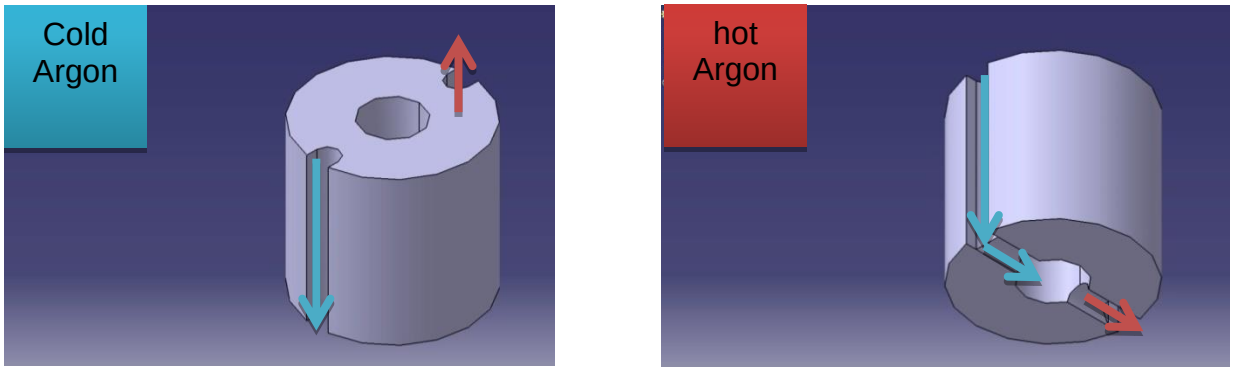

Fig. 18 – Details of the ceramic support (top and bottom view).

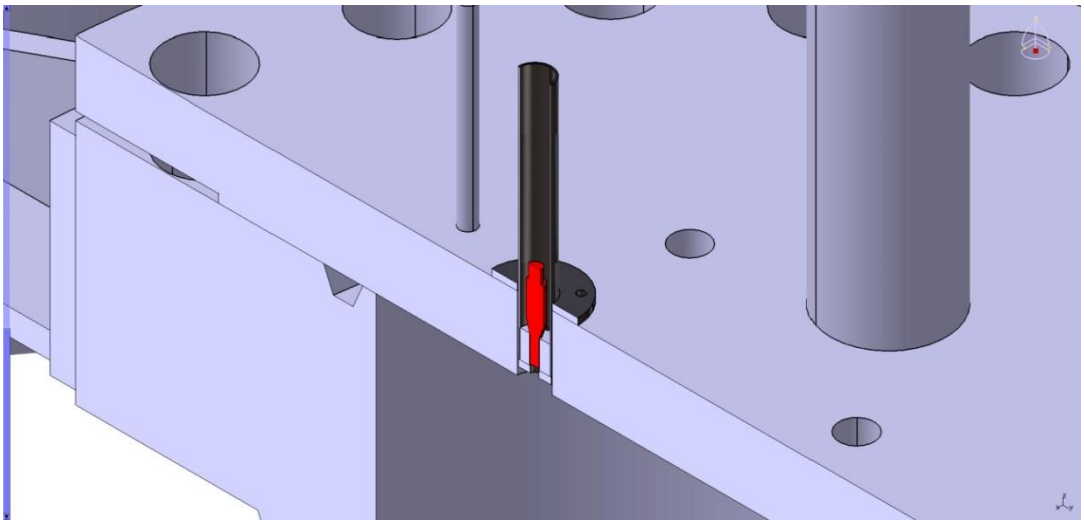

Fig. 19 – Assembly of the microphone and the Ar cooling system on LIFUS5/Mod3 top flange.

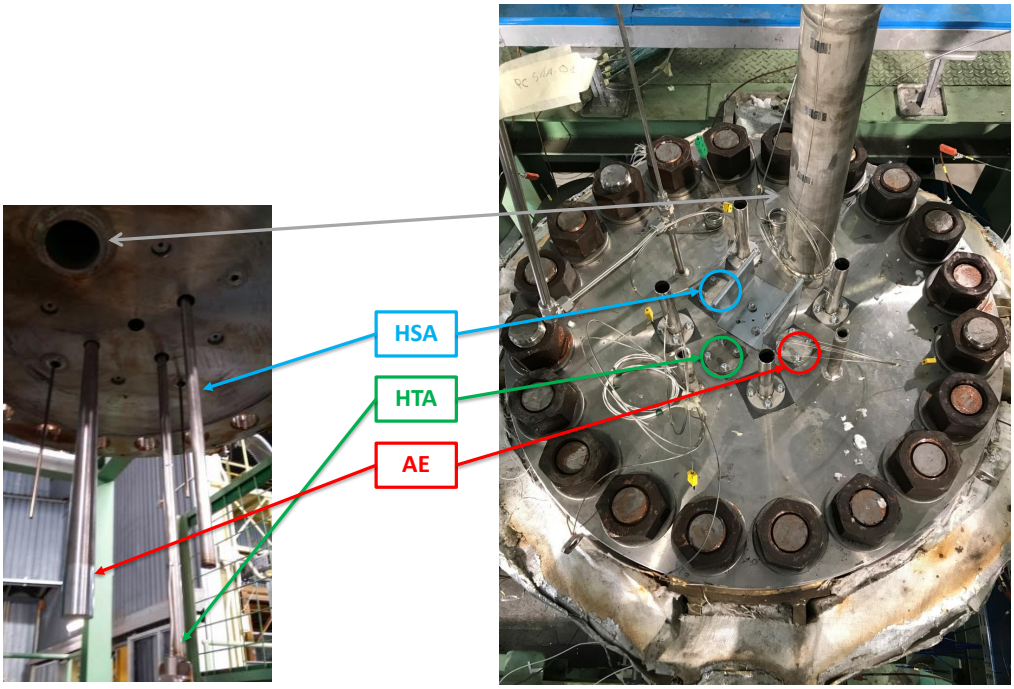

Fig. 20 – Penetrations of S1_A top flange and installation inside the vessel.

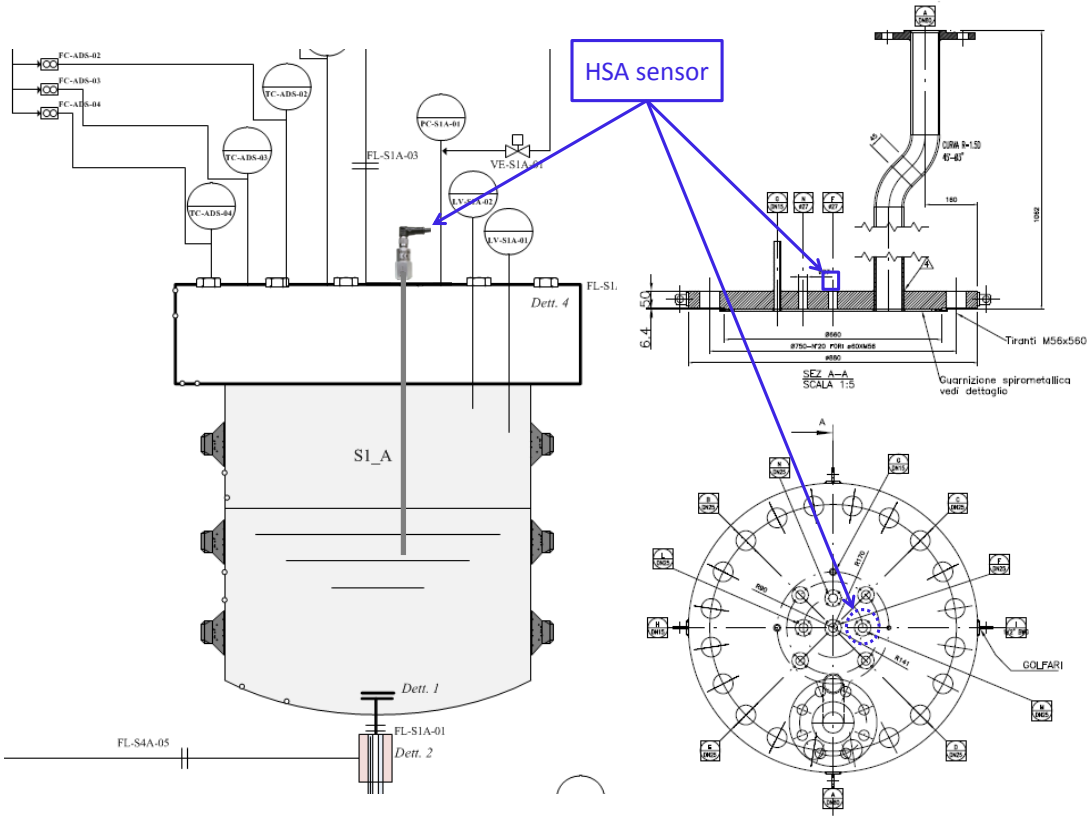

Fig. 21 – Layout of HSA sensor.

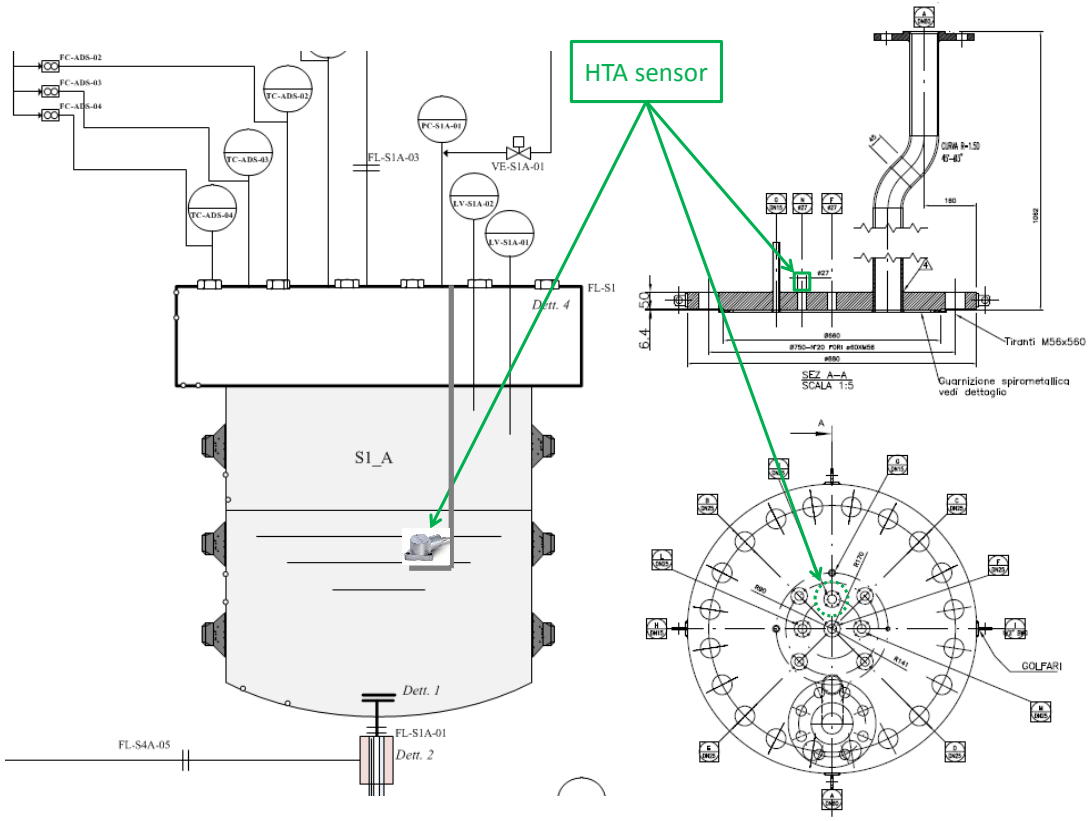

Fig. 22 – Layout of HTA sensor.

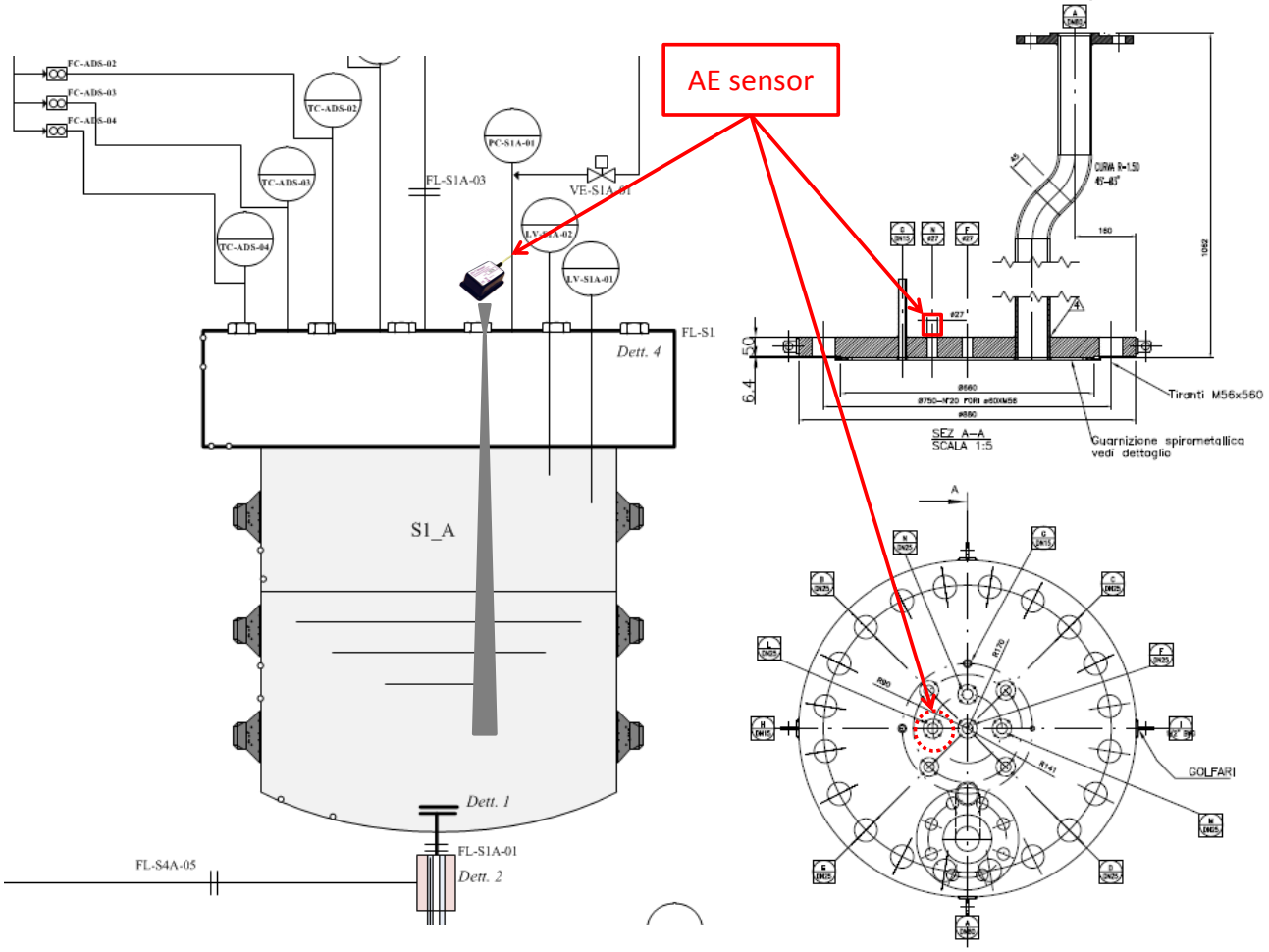

Fig. 23 – Layout of AE sensor.

Fig. 24 – Multichannel acquisition system DEWESOFT-SIRIUS®.

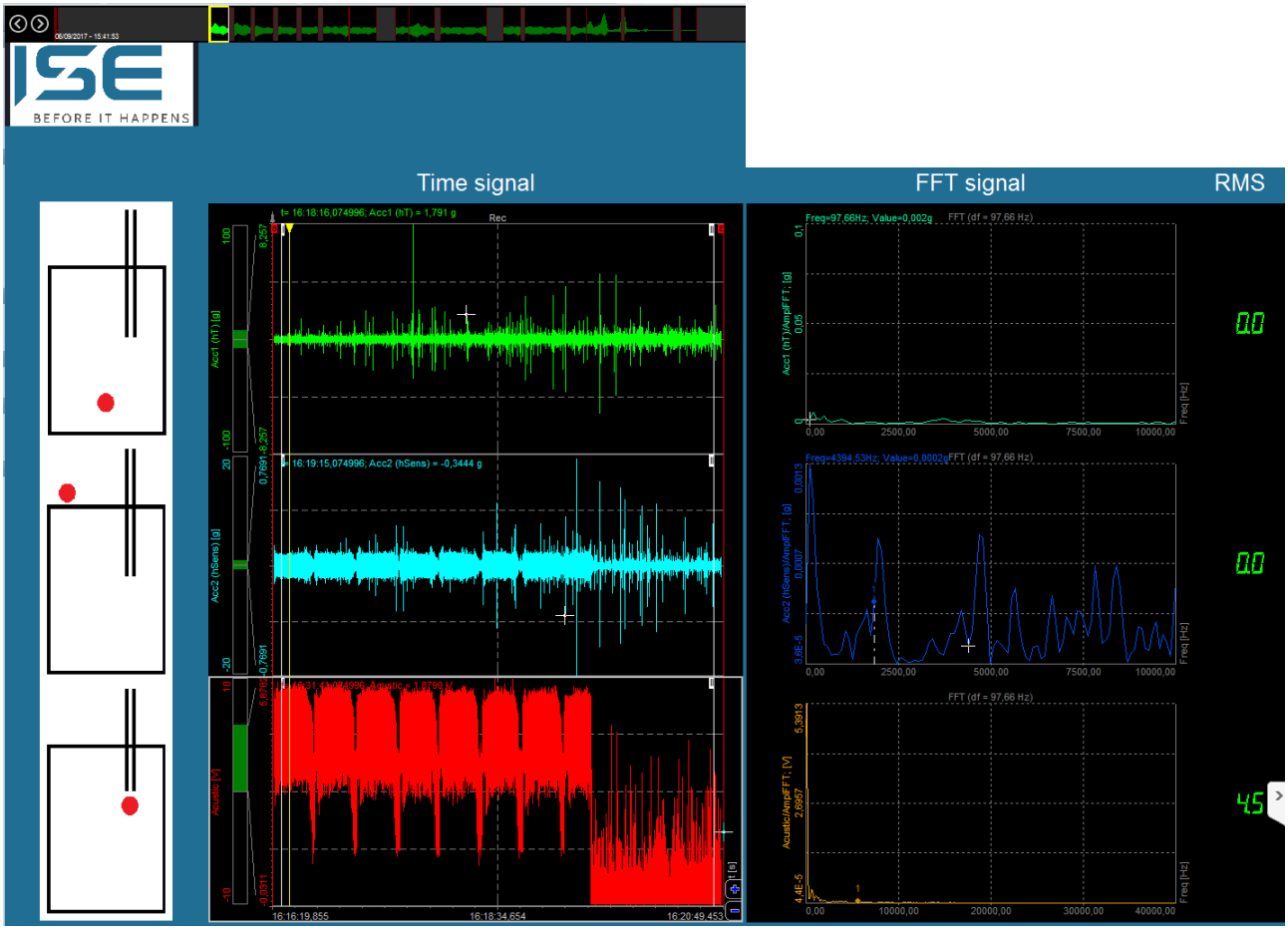

Fig. 25 – Software DEWESOFT X2SP10 for acquisition and data processing.

3 Description and analysis of Test C1.1_60

3.1 Time schedule of test execution

The time schedule of the test execution are summarized in Tab. 7.

3.2 The micro-holed injector and its characterization

3.2.1 Geometrical characterization

The characteristics of the N°21 micro-holed injector plate is shown in Fig. 26 (Ref. [3]). It has a mean diameter of 63 μm and an area of 3188.09 μm^2.

3.2.2 Experimental characterization prior to test

The day before the test, a characterization of the micro-holed injector plate was made in order to measure the mass flow rate of injected water and verify the behavior of the Coriolis mass flow meter. The injector N°21 was installed directly at the end of the injection line, discharging water towards the experimental hall. This phase was executed at atmospheric water temperature.

During the characterization, the Coriolis mass flow meter recorded a water mass flow of about 1500 g/h. This data is not in agreement with the result of the injected water recorded by the level meter LV-S2V-01. Indeed, the result between 2000 s and 7000 s (where the signal of LV-S2V-01 is stable, as shown in Fig. 27) highlights an average mass flow rate of 667 g/h and a total amount of water of 0.93 kg (Fig. 28). In order to investigate which is the more reliable data, RELAP5/Mod3.3 analyses were performed.

3.2.3 RELAP5/Mod3.3 characterization prior to test

The characterization of the water injection system has been investigated using RELAP5/Mod3.3 code ([7]). The nodalization is set-up modelling the actual geometry of LIFUS5/Mod3 injection line, as built. Fig. 29 provides the sketch of the nodalization. The LBE system (i.e. S1A) is modelled as a boundary condition, where pressure and temperature are imposed (i.e. 1.1 bar and 200 °C). No heat transfer is simulated between the LBE and the water systems.

Two simulations are performed in order to investigate the mass flow rate at the orifice of the water and Argon fluids in the conditions relevant for the experiment.

The injection pressure is set to 19 bar upstream the injection system. The temperature is varied stepwise in the range 15–275 °C, according with the trend reported in Fig. 30. The mass flow rate trends of Ar and water fluids are also reported.

RELAP/Mod3.3 analyses show that during the time interval of 0-2000 s (and therefore during the temperature stepwise of 0-50°C), the calculated water critical flow is about 535 g/h (Fig. 30). This data is slightly underestimated. However, it seems to confirm the record of the level meter instead of the not reliable Coriolis mass flow meter data. The amount of injected water in the same time interval is in the order of 0.3 kg (Fig. 31).

On the other hand, in the temperature range of 150-200 °C, RELAP5/Mod3.3 results show that the mass flow meter drops once the temperature of the fluid is closer to its saturation temperature. The two-phase chocked flow is established. In this time interval (9000-12000 s), the mass flow rate varies from 515 g/h to 305 g/h and the amount of injected water is in the order of 0.45 kg.

3.3 Analysis of the Test C1.1_60 and of the leak detection systems data

The Test LIFUS5/Mod3 C1.1_60 was executed on **September 6th, 2017 at 15:30**. It corresponds to test #1 of the test matrix (see Sect. 2.1).

The initial test conditions were achieved accordingly with the specifications with satisfactory accuracy. The water injection is executed using the valves VP-S2L-07 and VP-S2L-08 across the Coriolis flowmeter, and gas injection by means of VE-S2V-05. The acquisition system worked properly.

3.3.1 Thermal-hydraulic data analysis and interpretation

The main parameter time trends are reported in selected time scales from Fig. 32 to Fig. 40. In detail, Test C1.1_60 can be divided in 3 main phases:

1. **Gas injection phase**
2. **Water injection without LBE phase**
3. **Water Injection in LBE phase**

In the test series C, time 0 is not chosen accordingly with specific time event because of the peculiarity of each test. Therefore in test C1.1_60, time 0 s is assumed at 15:30:01, when the acquisition system is activated. The acquisition time lasts 24000 s.

In the first phase of the test, gas was injected through VE-S2V-05 in order to prevent the blockage of the micro-holed injector plate. The facility achieved the hot standby conditions (temperature of the S1A vessel higher than 180 °C) in 566 s.

The Start of Injection (SoI), chosen when the injection switched from gas to water, occurs at 2915 s by means of VP-S2L-07 valve. This is the second phase of the test, when the water is injected in S1A empty vessel. During this phase, the ADS and accelerometers acquisition system were activated.

The third phase is chosen by the user when the LBE level is stable in S1A (signal of stable level in S4A accordingly with the continuum level meter LV-S4A-03). At time t = 6437 s, the Start of the Test (SoT) occurs. During this phase, which is concluded at time 11507 s, the Coriolis mass flow meter records an injected mass flow rate of about 700 g/h, while the level measured in S2V by LV-S2V-01 recorded a decrease from 1191 to 1141 mm. The decrease of 50 mm in level leads to a calculated injected of water of about 0.44 kg in 5070 s, and an average mass flow rate of 312 g/h. The experienced data confirm the RELAP5/Mod3.3 results.
The third phase ends with the drainage of the LBE from S1A interaction vessel towards the storage tank. Valve VP-S4A-01 opens at t = 11499 s and closes at t = 11867, when the LBE drain procedure ends. Meanwhile, the water continues to be injected up to t = 11888 s when the injection switched from water to gas. During this period, the ADS and accelerometer acquisition turn off.

Concerning the temperatures, TC-S1A-01 shows a sudden decrease probably due to the mixing of water, injected at lower temperature, and LBE during the filling procedure. After that, both of the thermocouples install in the interaction vessel S1A show a rapid increase of about 10 °C. Indeed, the LBE stored in S4A is maintained at temperature of 200 °C, but

the filling pipe reached about 250 °C. During the filling procedure, the LBE is heated up, and locally brings to an increase of temperature in the interaction vessel.
During the test (between SoT and EoT) the thermocouples in the injection line from TC-S2L-03 to TC-S2L-06 recorded a maximum temperature of 100 °C. The water heating occurs in the last section of the injection line. TC-S2L-07 recorded a maximum temperature of 185 °C, then it dropped down accordingly with the test execution (FS-S2L-07 switch off), and TC-S2L-08, installed just before the injector, recorded a maximum temperature of 195 °C (injector cooling system by Argon gas switched off). During all the transient, the injected temperature is lower than the saturation temperature at 19 bar (211.64 °C).

Tab. 7 – Test C1.1_60, time schedule of test execution.

#	Time	Timing	Phase	Description	Signal
Characterization Phase (05.09.2017)					
1	15:21:11	--	Characterization starts	Water injection on	VP-S2L-07
2	16:59:11	--	Characterization ends	Water injection off	VP-S2L-07
Experimental Test (06.09.2017)					
3	09:22:08	--	Gas injection on		VE-S2V-05
4	10:12:48	--	Facility conditioning starts	Heat-up procedure starts	CS-S1A-01
5	15.30:01	t = 0	Starting acquisition		
6	15:39:27	t = 566	Facility conditioning ends	Hot standby conditions achieved (T > 180°C)	TC-S1A-01 TC-S1A-02
7	16:18:36	t = 2915	Start of Injection – SoI	Water injection	VP-S2L-07
8	16:29:13	--	Leak detection systems on (ADS)		First .txt file
9	16:35:07	t = 3906	Filling	LBE fill procedure starts	VP-S4A-01
10	16:39:10	t = 4149	Leak detection systems on (HSA,HTA,AE)		UDV-ADS-A
11	17:17:15	t = 6434	Filling	LBE fill procedure ends. S1A filled	VP-S4A-01
12	17:17:18	t = 6437	Start of Test – SoT	S1A filled in steady state	LV-S4A-03
13	18:41:40	t = 11499	Draining	LBE drain procedure starts	VP-S4A-01
14	18:41:48	t = 11507	End of Test – EoT	S1A filled in steady state	LV-S4A-03
15	18:47:48	t = 11867	Draining	LBE drain procedure ends	VP-S4A-01
16	18:48:09	t = 11888	End of Injection – EoI	Water injection off	VP-S2L-07
17	19:28:05	--	Leak detection systems off (ADS)		Last .txt file
18	21:20:24	t = 21023	Gas injection off		VE-S2V-05
19	21:35:24	t = 21923	Leak detection systems off (HSA,HTA,AE)		UDV-ADS-A
Conditioning Phase (07-08/09/2017)					
20	13:08:03 07/09/2017	--	Facility shut-down starts	Heating wires switched-off	CS-S1A-01
21	09:21:30 08/09/2017	--		Water system depressurization and emptying	VE-S2V-03
22	09:30:00 08/09/2017	--	Facility shut-down ends	Facility cold (T < 60 °C)	TR-S1A-1A TR-S1A-1B

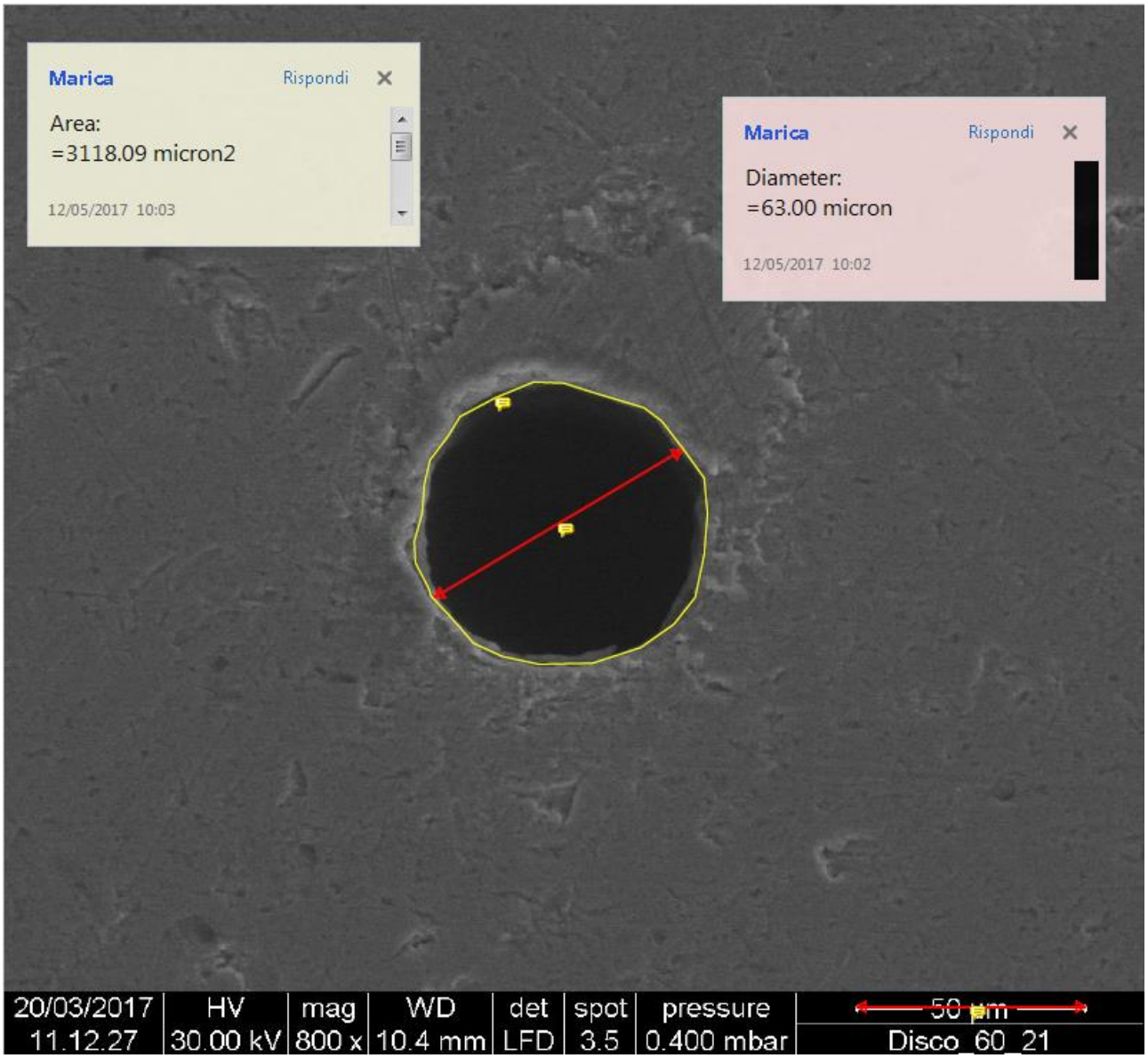

Fig. 26 – Characteristics of N°21 micro-holed injector plate.

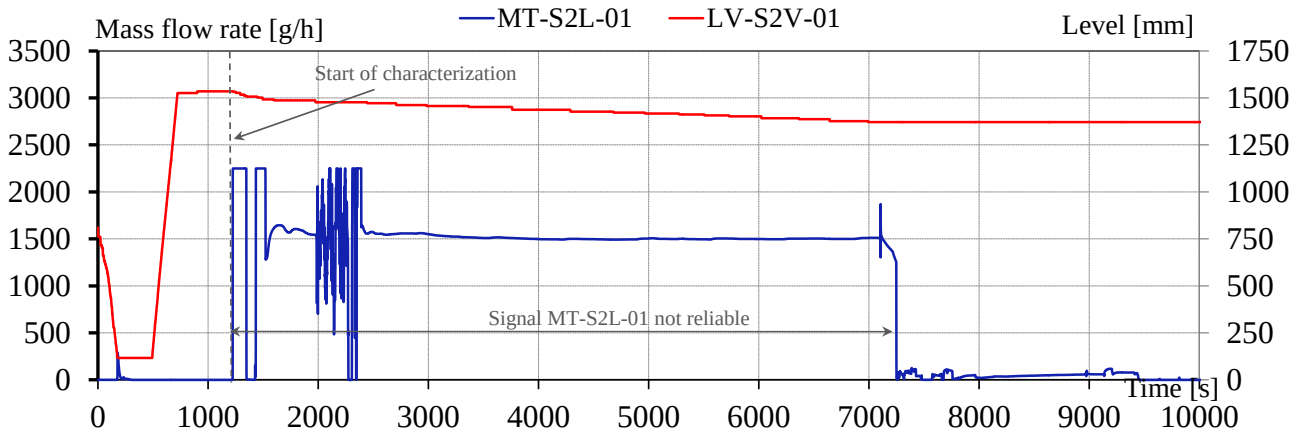

Fig. 27 – Characterization of orifice N°21 prior to test: S2V level and mass flow rate.

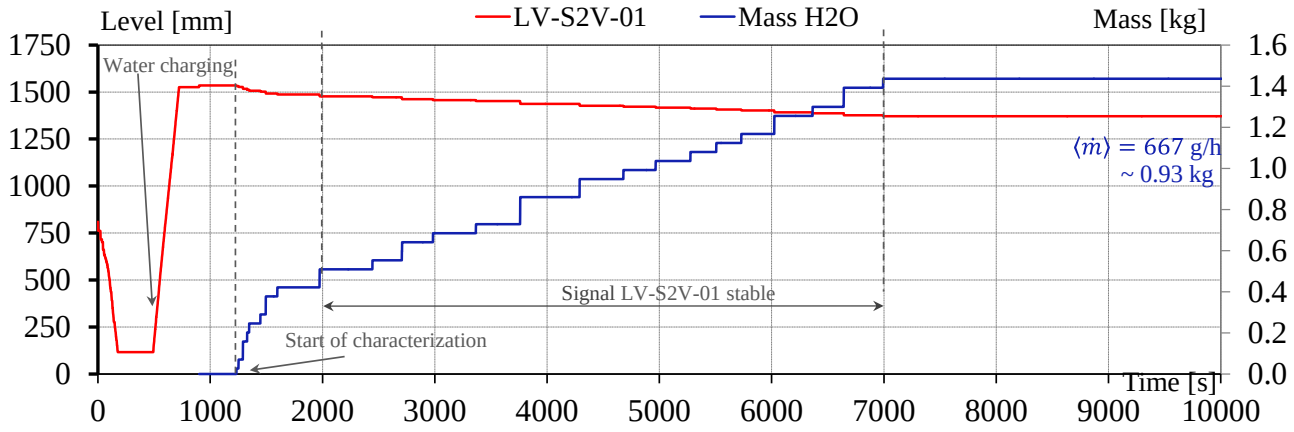

Fig. 28 – Characterization of orifice N°21 prior to test: S2V level and calculated integral mass.

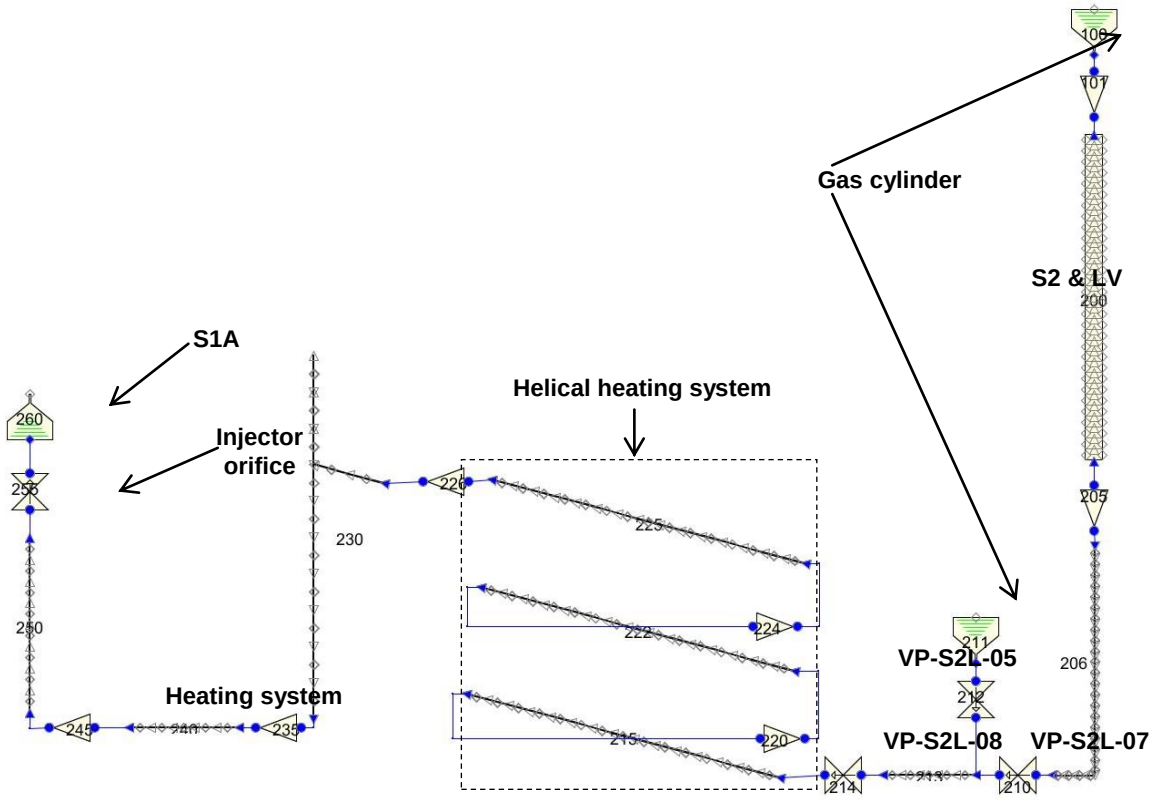

Fig. 29 – RELAP5/Mod3 nodalization of LIFUS5/Mod3 injection line

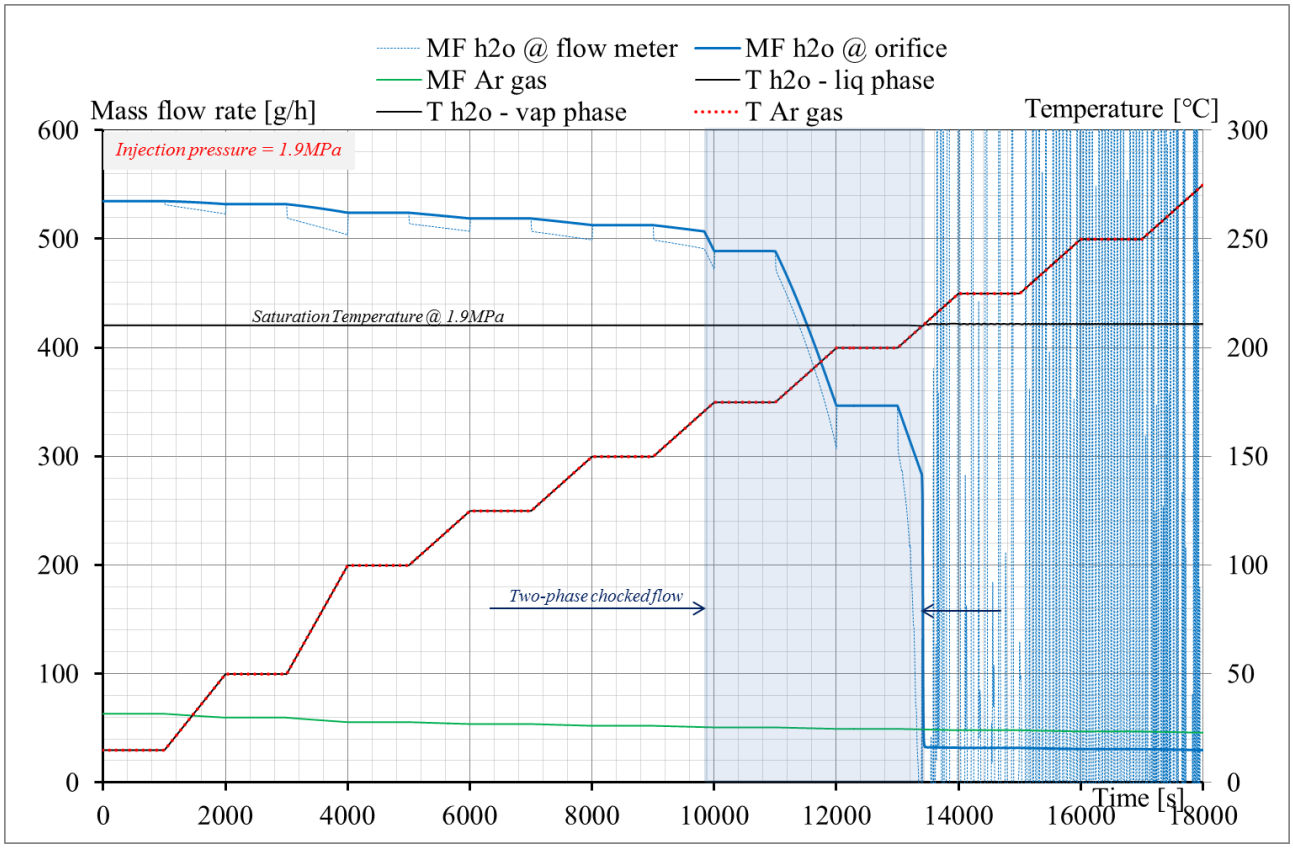

Fig. 30 – Orifice N°21: calculation of the Ar and H_2O mass flow rate through the orifice at P=1.9 MPa and fluid temperatures between 15-275°C

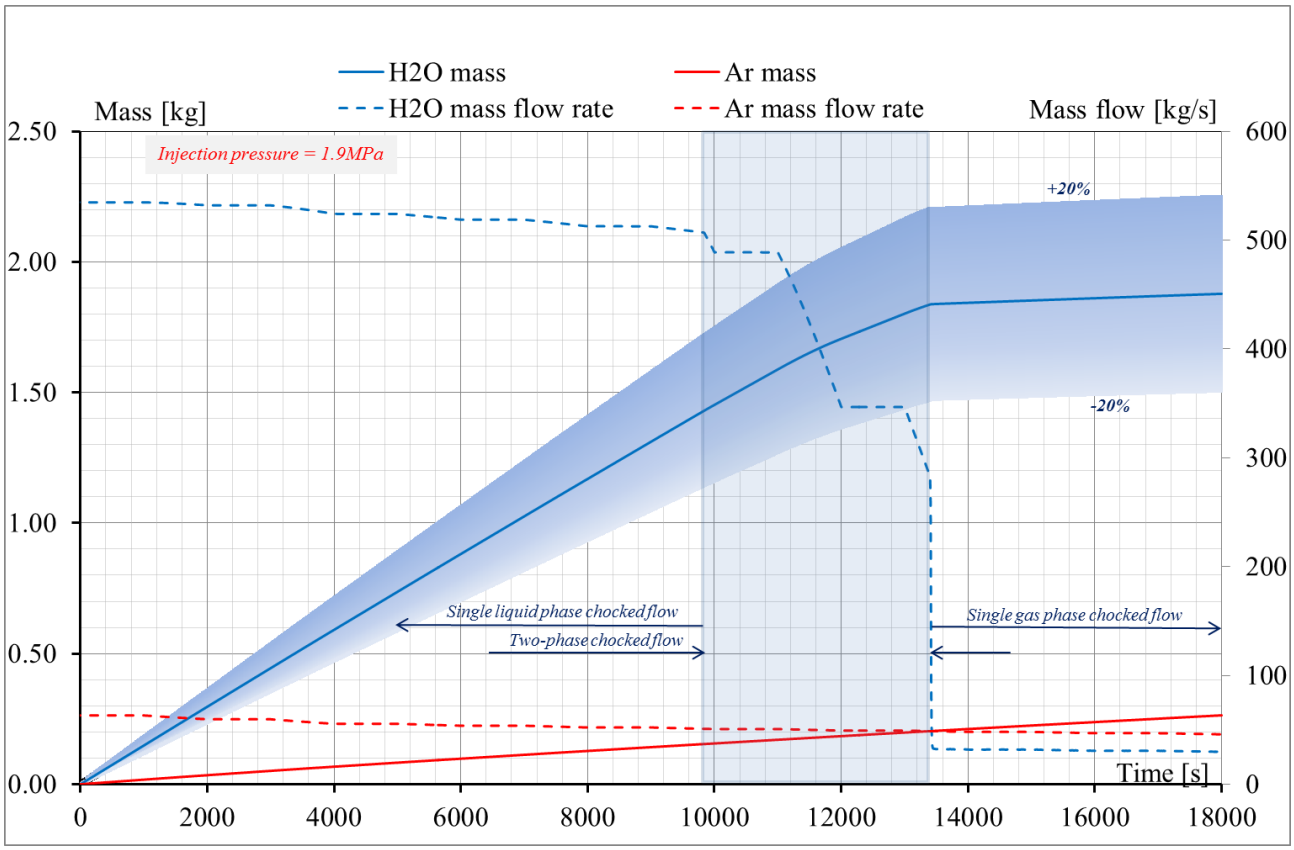

Fig. 31 – Orifice N°21: calculation of the Ar and H_2O integral mass injected through the orifice at P=1.9 MPa and fluid temperatures between 15-275°C

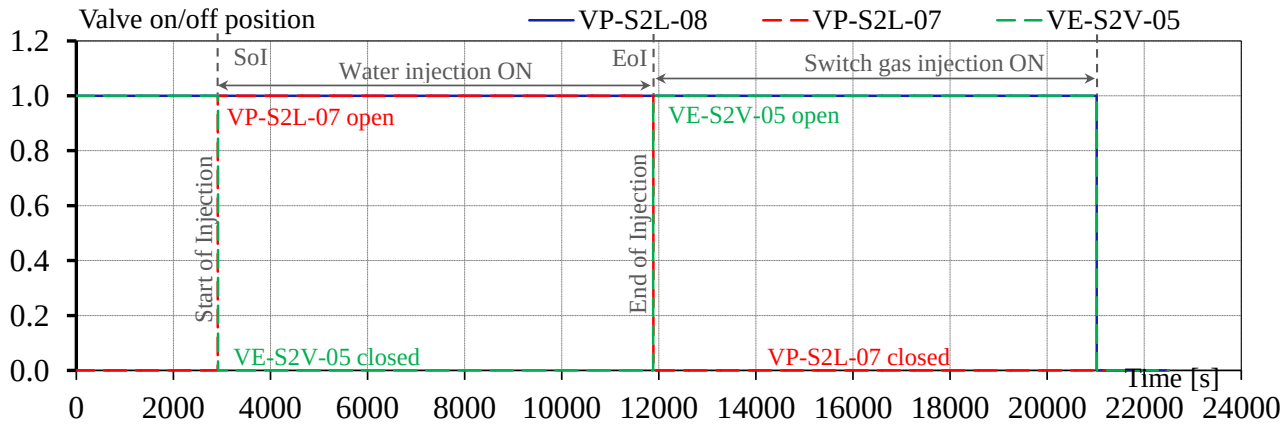

Fig. 32 – Test C1.1_60, valve VP-S2L-07, VP-S2L-08 and VE-S2V-05 positions.

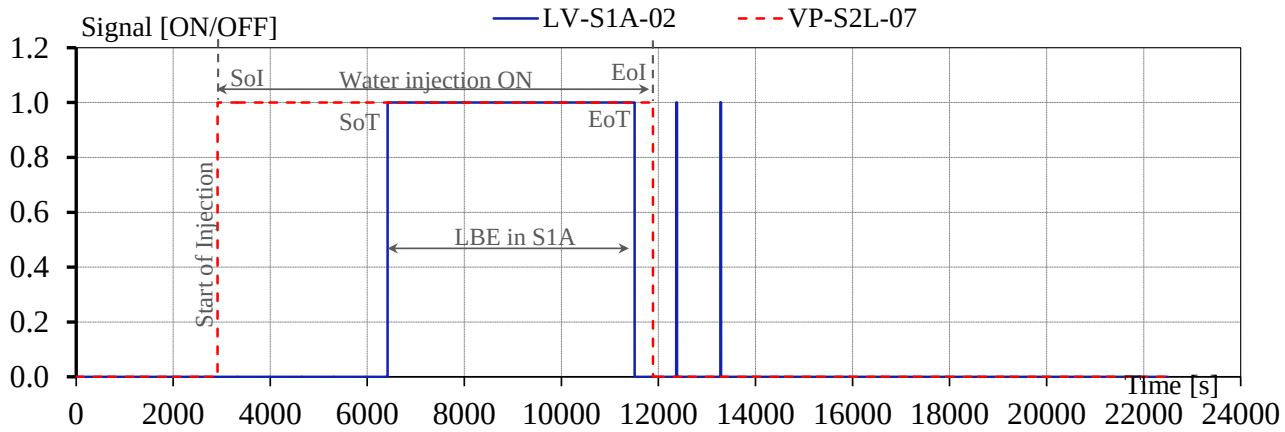

Fig. 33 – Test C1.1_60, valve VP-S2L-07 and S1A low level positions.

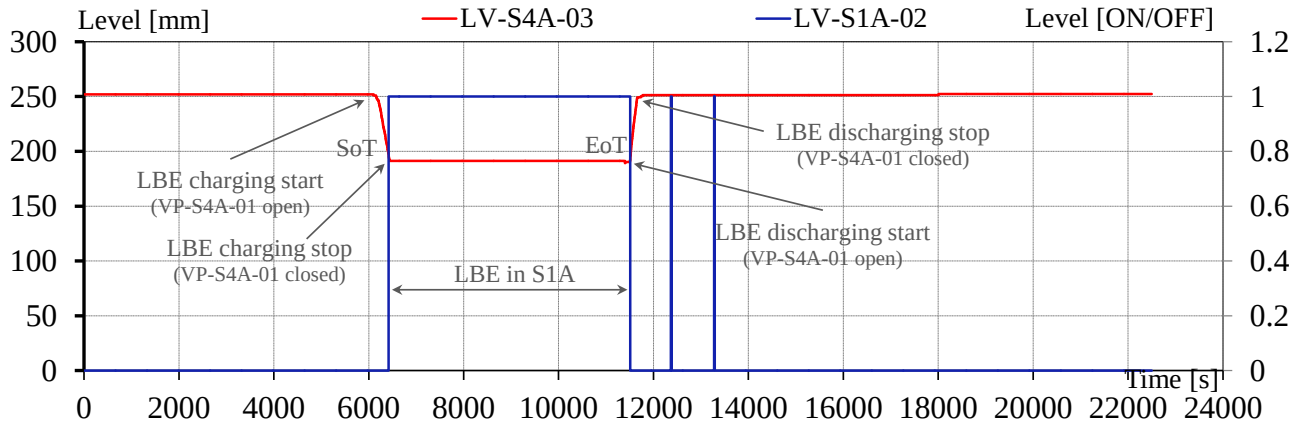

Fig. 34 – Test C1.1_60, continuum level in S4A and low level in S1A.

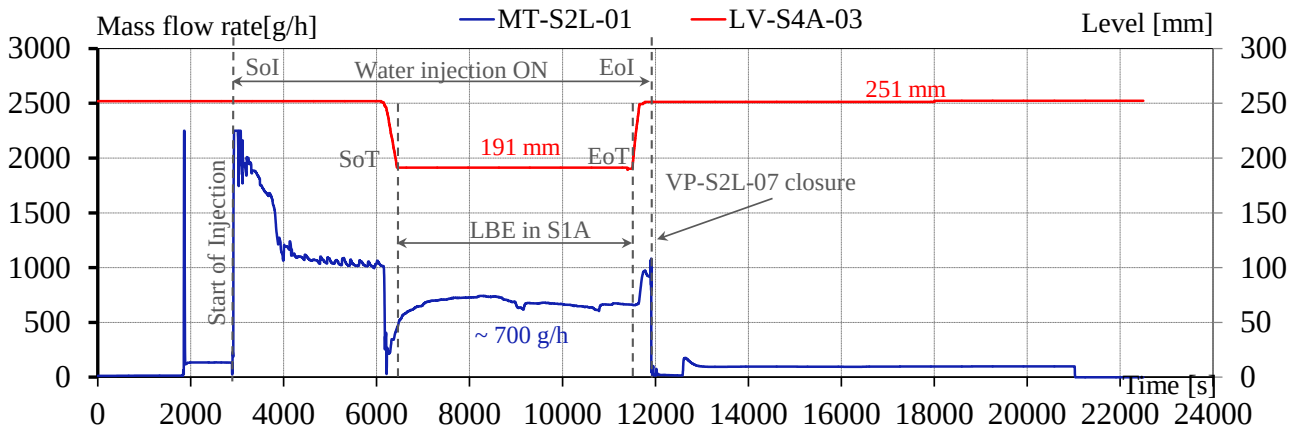

Fig. 35 – Test C1.1_60, mass flow rate in injection line and LBE level in S4A time trends.

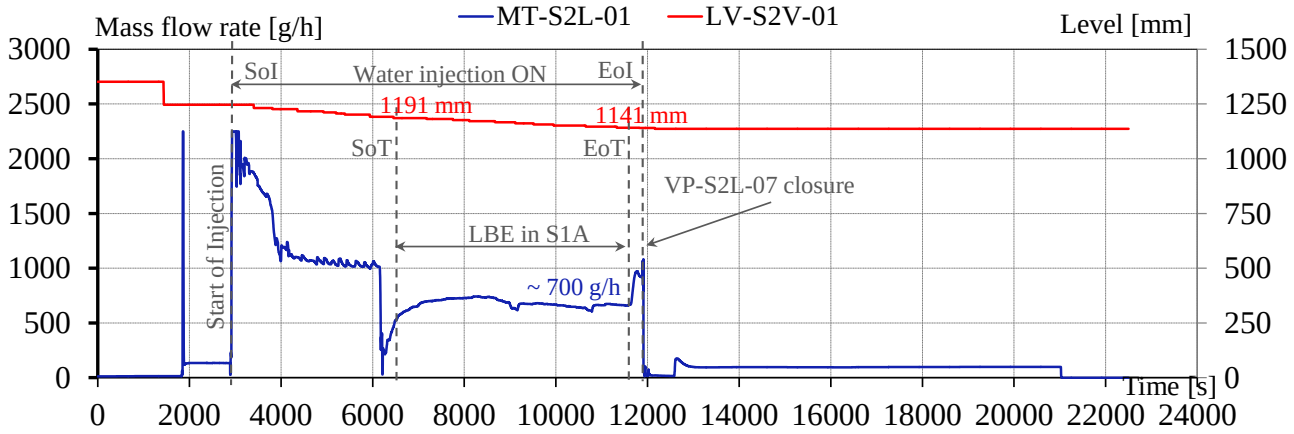

Fig. 36 – Test C1.1_60, mass flow rate in injection line and water level in S2V time trends.

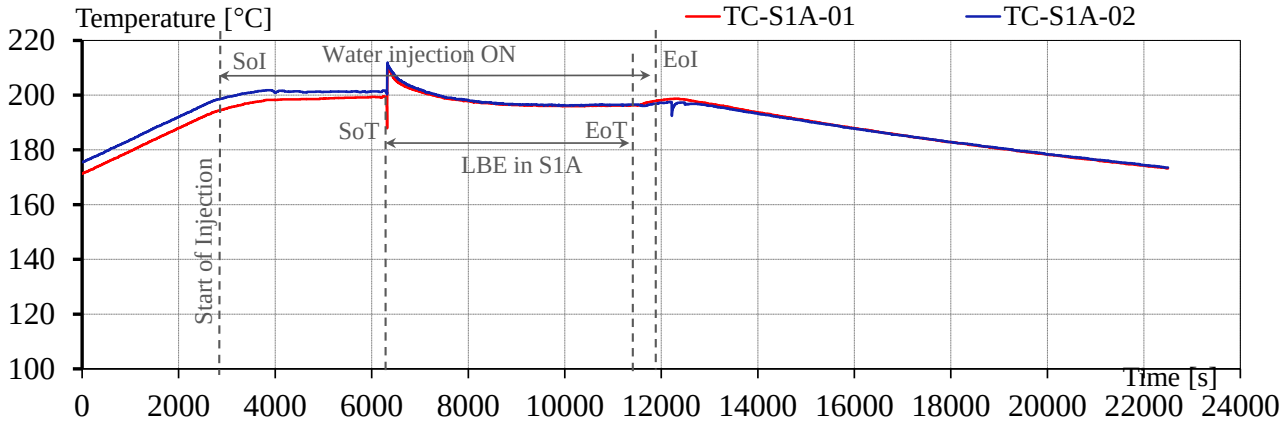

Fig. 37 – Test C1.1_60, temperature time trends in the interaction vessel.

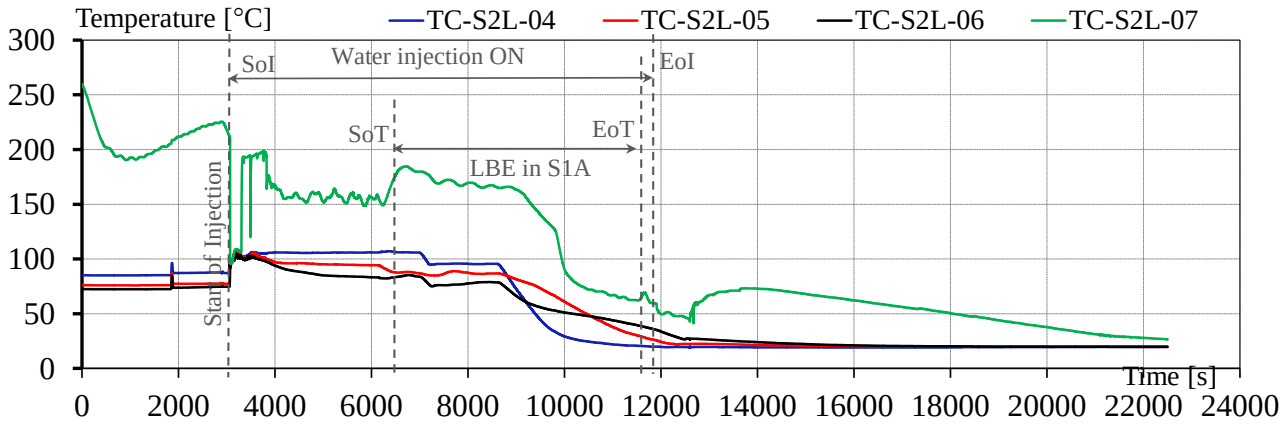

Fig. 38 – Test C1.1_60, temperature time trends in injection line.

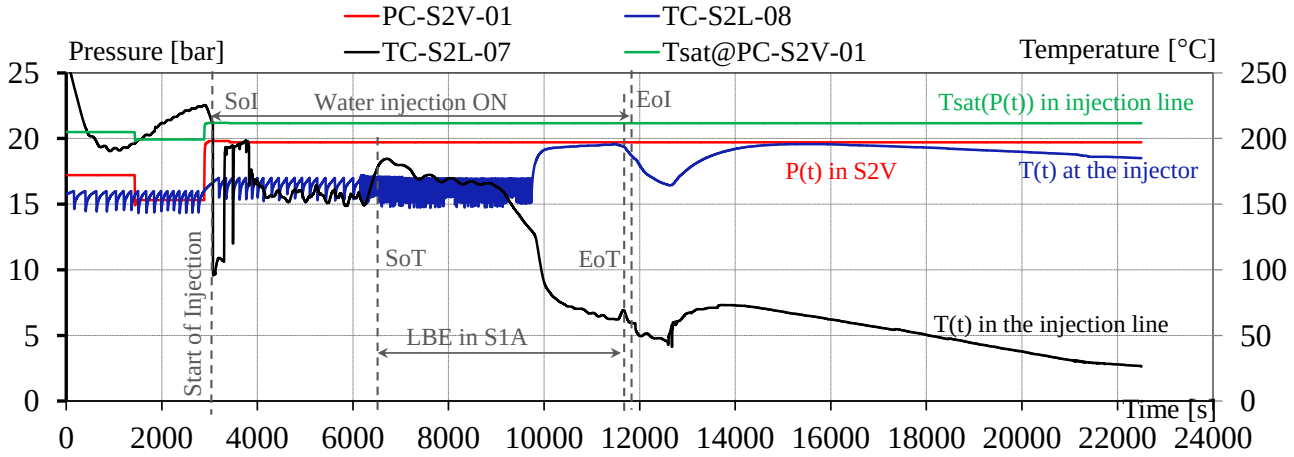

Fig. 39 – Test C1.1_60, pressure and temperature time trends in injection line.

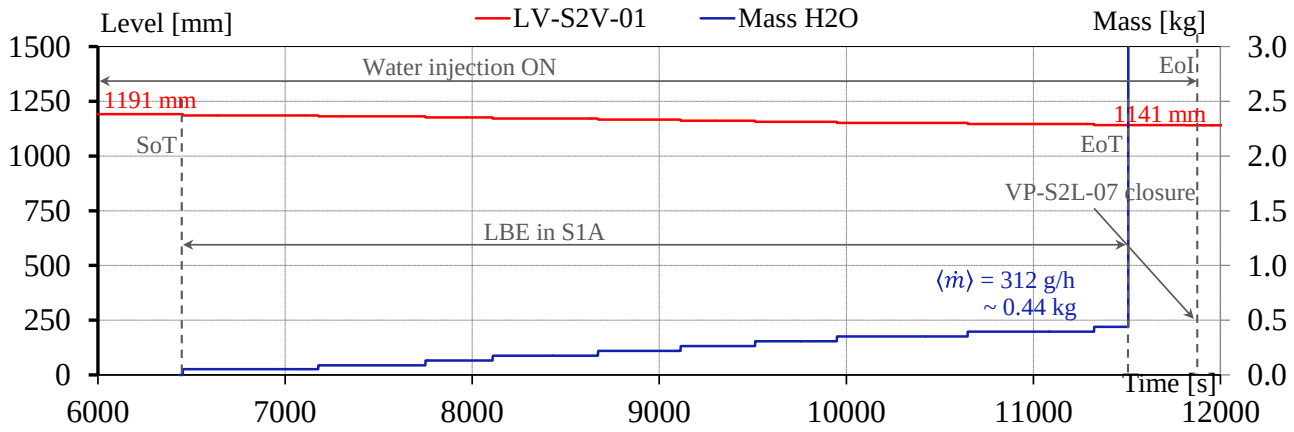

Fig. 40 – Test C1.1_60, water level in S2V and integral value of injected water time trends.

3.3.2 Analysis of acoustic detection system data and interpretation

3.3.2.1 Introduction

The main target of this application is to correlate the dimension of the orifice with the sound pressure wave generated inside the tank. To get this result the main idea is to check the frequency response of the sound pressure waves and to correlate the frequency change to the diameter of the orifice. The chosen platform is a PC based on GNU/Linux and an ADC with a sampling frequency of FS = 20 kHz. All the data during the test are stored on the PC as raw data (not elaborated) available for post process analysis.

3.3.2.2 Data

During a single test a lot of data are recorded. For a test of about 2 hour there are:

$$2\ (hours)\ x\ 3600\ (seconds)\ x\ 20000\ (samples)\ x\ 5\ (channels) = 720 * 10^6 values$$

This set of data is large for a single file. Moreover, the post processing would be prohibitive if they are recorded in a single file. For this reason, the data are stored in a series of *.txt files with a specific name encoded to guarantee the data integrity. Each filename has the following labelling approach:

YYYY-MM-DD-HH-MM-SS-acquisizione.txt

The file contains 6 columns, respectively:

Data-time	Channel_1	Channel_2	Channel_3	Channel_4	Channel_5
2017/09/06 19:28:07.659907;	0.026093;	0.027924;	0.019074;	0.028840;	0.029145;

each field is separated by semicolon (“ ; ”) in order to ensure an easy file importation procedure.

Inside the file, the field “Data-time” is written in the format: YYYY/MM/DD HH:MM:SS.XXXXXX, so for each row the reference time is reported. The vectors “channel_*” report the values of the recorded signal, which is an electric voltage in the range of ±10 V.

Each row represents a single time step, and the number of rows for each file is fixed to 40000: therefore each one has 2 seconds of data. The dimension of each single file is about 3.1 MB.

The data acquired during test C1.1_60 are:

Data	Channel_1	Channel_2	Channel_3	Channel_4	Channel_5
2017-09-06	From 0 to ~5000[s]	-	From 0 to ~13500[s]	-	-

The total number of files are 5368, for a total memory size of 16278 MB of raw data.

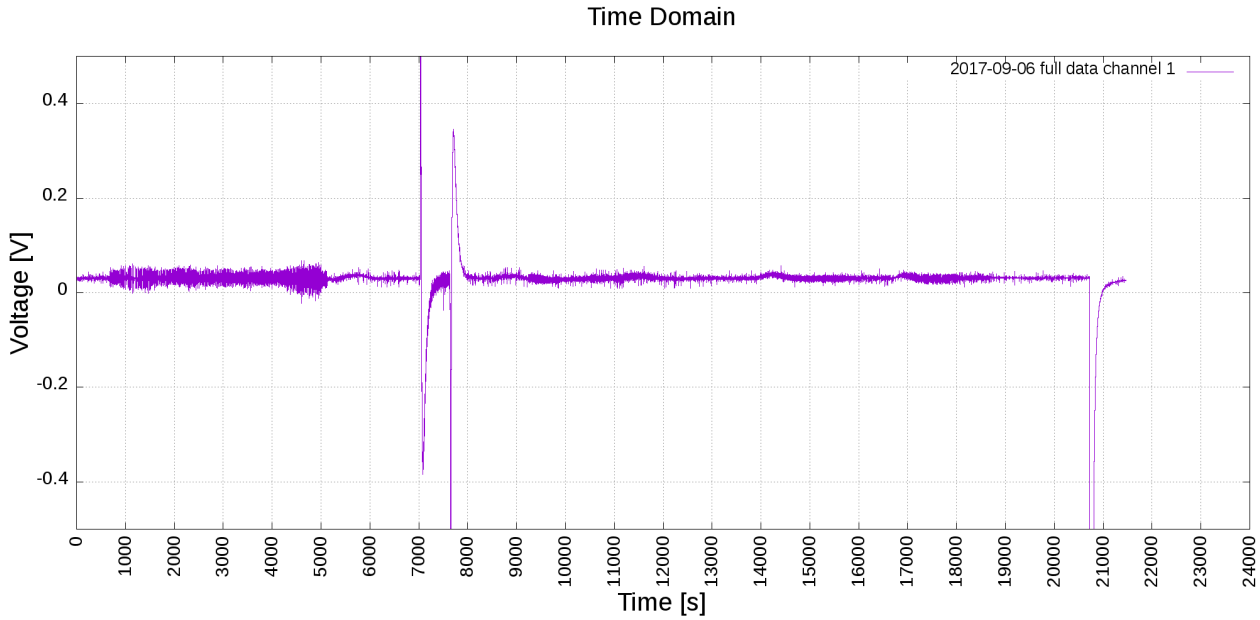

Fig. 41 – Test C1.1_60, raw data channel 1 [time domain].

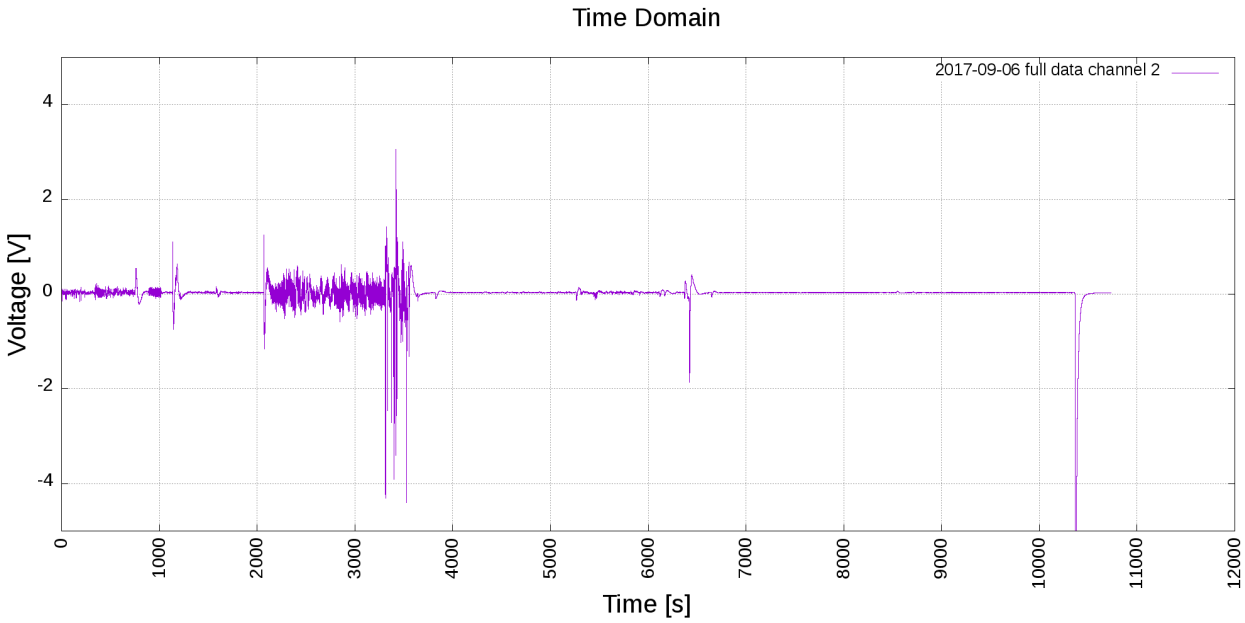

Fig. 42 – Test C1.1_60, raw data channel 2 [time domain].

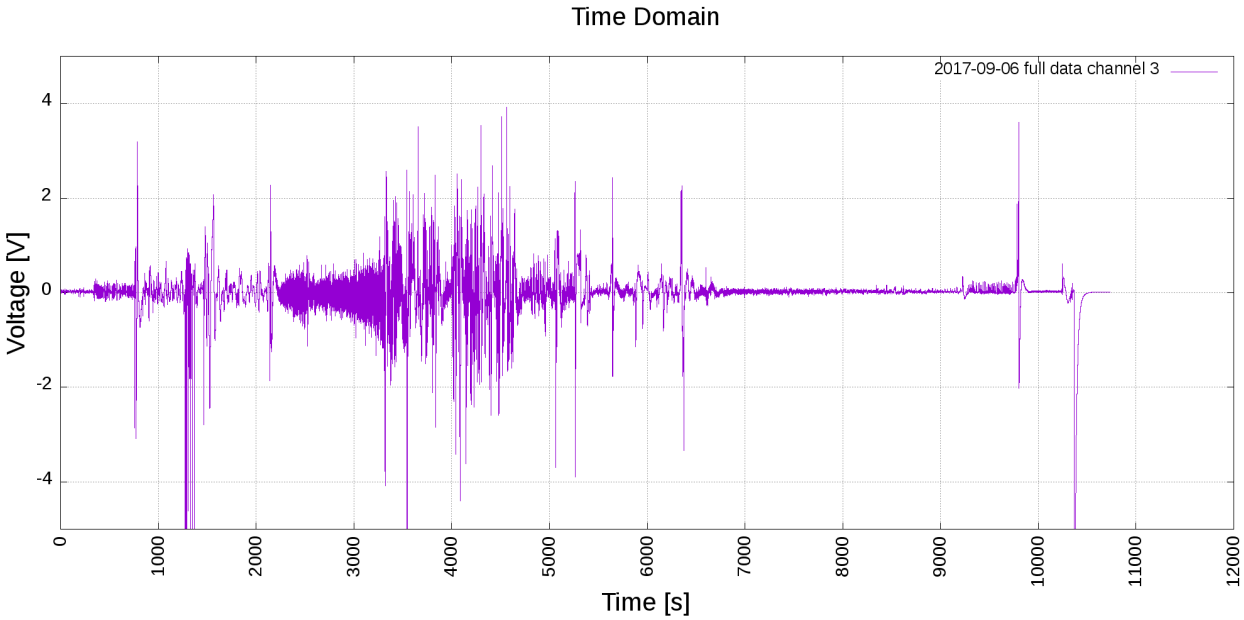

Fig. 43 – Test C1.1_60, raw data channel 3 [time domain].

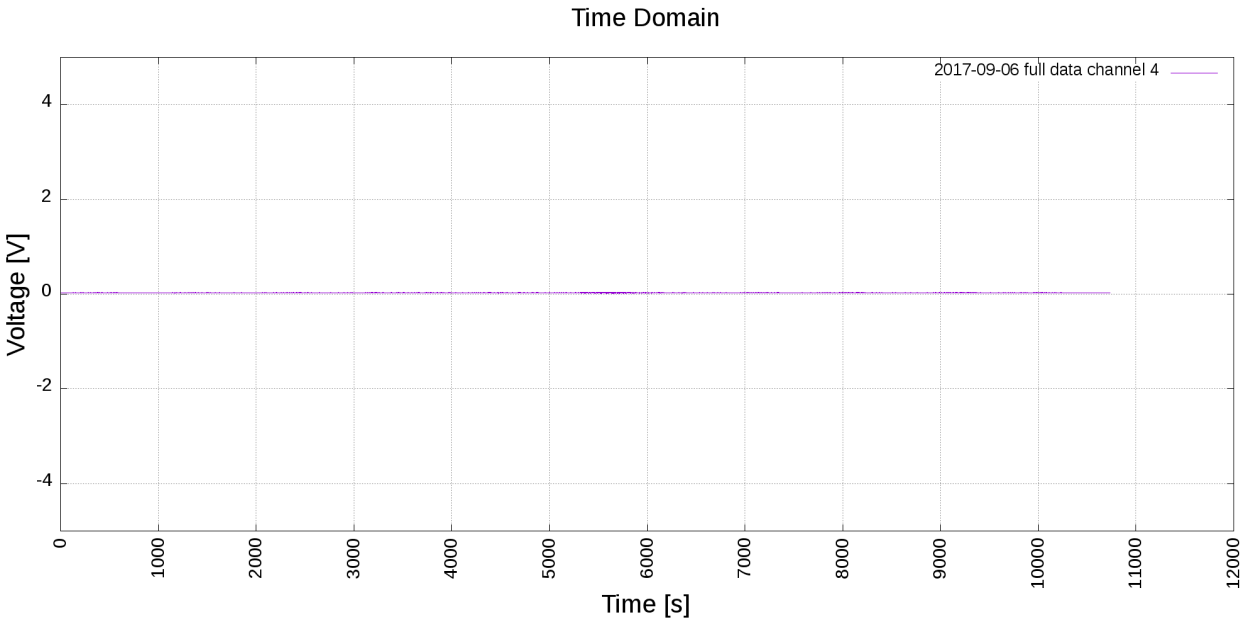

Fig. 44 – Test C1.1_60, raw data channel 4 [time domain].

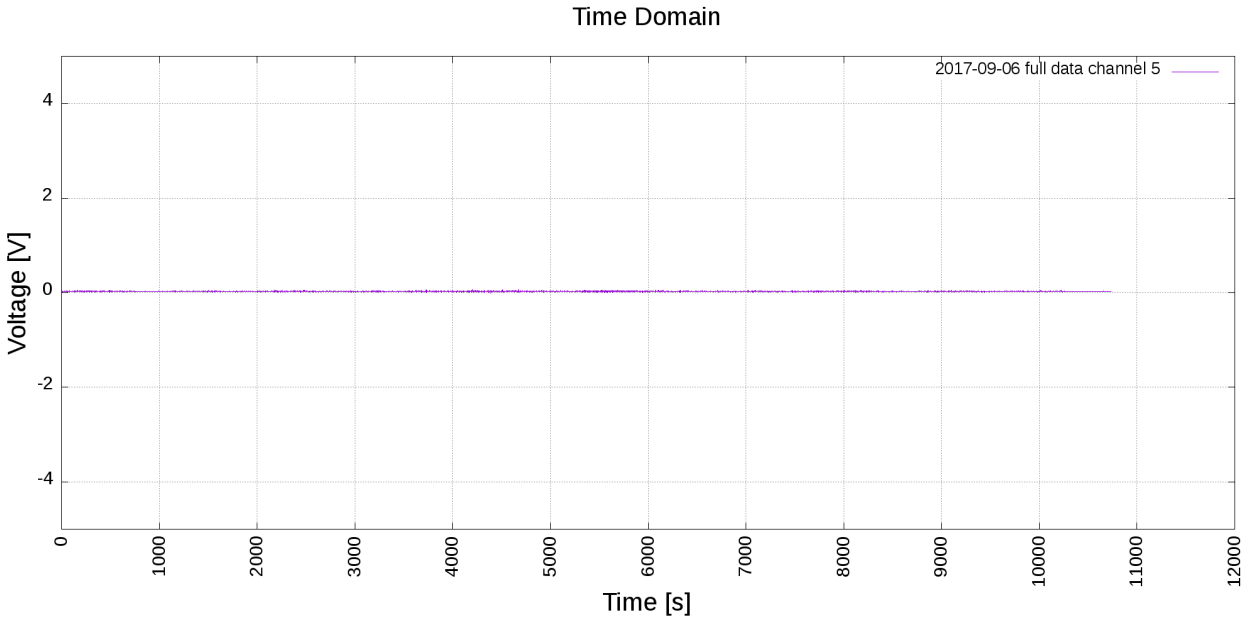

Fig. 45 – Test C1.1_60, raw data channel 5 [time domain].

3.3.2.3 Analysis

The analysis of the samples is divided into two procedures:

1. FFT transforms;
2. SLICING analysis.

Two programs C++ were developed for the post-processing of data and the analysis.

3.3.2.3.1 FFT transforms

The first step concerns the FFT computing of the stored data by the library FFTW (http://www.fftw.org/). The developed code uses this library to calculate the FFT with a certain frequency (defined FFT@fs = 100 Hz).

The stored data are sequentially loaded and continuously transformed in order to have a series of FFT files from which extracting the frequency spectrum of the bubbles.

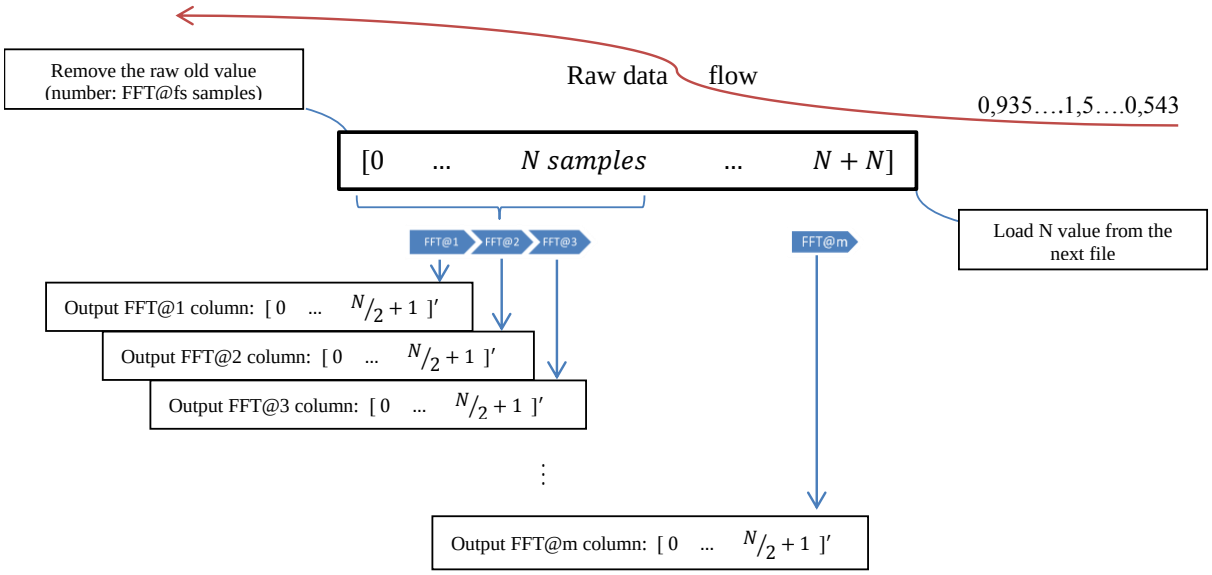

Fig. 46 – Test C1.1_60, FFT computing procedure.

Each computed file represents the FFT of a INPUT vector of N=20000 samples loaded from the raw data (time domain). The FFT output file is composed of N/2+1 values representing the energy in db from 0 (continuous component) to the frequency fs/2 = 10 kHz (Hz in the frequency domain). The output files, including the FFT, are stored to the hard drive with the name:

AAAA-MM-GG-HH-MM-SS-fft_01234_ch_n.txt

This means that for each raw file there are 2 x FFT@fs(100) number of files within the same timestep; at the end of the name is added a suffix: “-fft_” and a progressive number related to the specific FFT translation.

3.3.2.3.2 SLICING analysis

Once the FFT transformed files are available, the second procedure “the SLICING” can be started. The first step is to load the output FFT files previously computed into a matrix:

$$M_{ch_i} = \begin{bmatrix} FFT@1[0] & \cdots & FFT@1[N/2+1] \\ \vdots & \ddots & \vdots \\ FFT@m[0] & \cdots & FFT@m[N/2+1] \end{bmatrix} \quad for\ i = 1\ to\ 5\ (channel)$$

m represents the number of computed FFT (number of raw file x FFT@fs).

Then, for each row of the matrix M_{ch_i} the energy values are calculated for each slice. The dimension of the slice id defined as “$\text{slice}_{\text{dim}}$” that represents the dimension of a subvector made by the sum of the single components:

$$\text{slice}_{\text{dim}} = \left\lfloor \frac{N/_2 + 1}{num\ of\ slice} \right\rfloor$$

Fig. 47 – Test C1.1_60, FFT energies file with reported the slice.

The computed values for each slice are saved in a matrix:

$$\text{num_of_slice} \rightarrow \quad \downarrow \text{FFT files} \quad M_{sl_i} = \begin{bmatrix} slice@1[0] & \cdots & slice@1[num_of_slice - 1] \\ \vdots & \ddots & \vdots \\ slice@m[0] & \cdots & slice@m[num_of_slice - 1] \end{bmatrix} \quad for\ i = 1\ to\ 5(channel)$$

named: “Energies Slice Matrix” M_{sl_i}.

The total energy for each slice is the sum of its internal energies components:

$$slice@1[j] = \sum_{i=1}^{slice_{dim}} pos[_{(slice_{dim}*j)+i}] \quad evalueted\ for \begin{cases} FFT@file = 1 \\ j = 0 \end{cases}$$

Progressively, at the end of the computing of every row of the matrix $\text{M}_{\text{sl}_\text{i}}$, for each slice the difference between the actual total energy for this slice and the minim energy value for the corresponding column is calculated. If the difference between two values is greater

than the value (obtain experimentally) Δ_{t_en} (delta_threshold_energy), the matrix M_{var_i} is filled with:

$$\text{for i} = 0 \text{ to num_of_slice} \begin{cases} \text{if } \left(\Delta_{t_{en}} \geq \text{slice@1[i]} - \text{slice[i]}_{min}\right) \text{ then} \\ \quad \text{var@1[i]} = 1 \\ \quad \text{else} \\ \quad \text{var@1[i]} = 0 \end{cases}$$

Then for each element of the matrix M_{sl_i} it is created a matrix M_{var_i} named: Variation Matrix defined as:

$$M_{var_i} = \begin{bmatrix} \text{var@1[0]} & \cdots & \text{var@1[num_of_slice} - 1] \\ \vdots & \ddots & \vdots \\ \text{var@m[0]} & \cdots & \text{var@m[num_of_slice} - 1] \end{bmatrix} \quad \text{for i} = 1 \text{ to } 5(\text{channel})$$

As last step, we can browse each column row by row of M_{var_i} and check the energy peak of the transition given by the bubble. Each peak detected belongs the column and it is given by the transition of a bubble.

3.3.2.4 Results

3.3.2.4.1 Bubble Frequency Analysis

In the following, two pictures report the FFT plot of two different time windows:

1. 17:30:06,50: FFT without the bubble;
2. 17:30:07,02: with the energy of the bubble;

both acquired from the microphone on the channel 1.

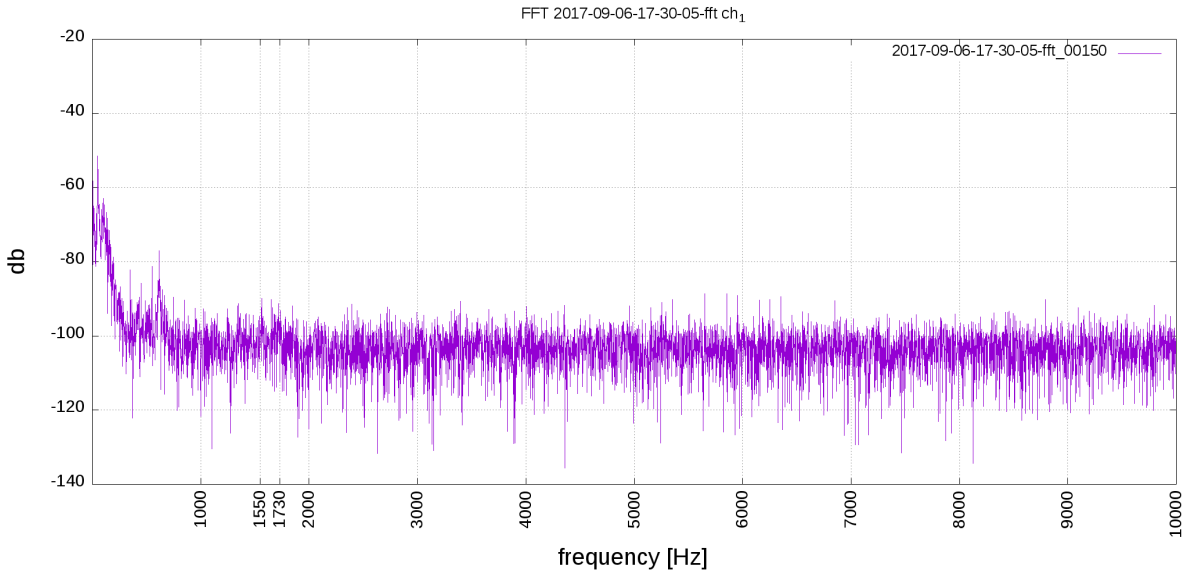

Fig. 48 – Test C1.1_60, details without bubble @time 17:30:06,50 on channel 1.

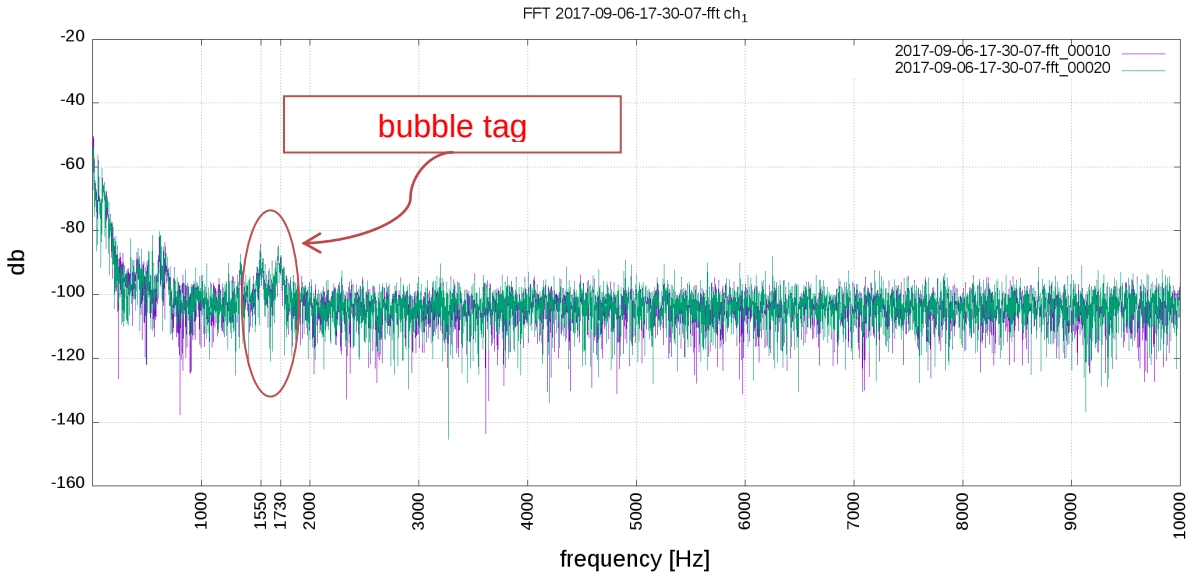

Fig. 49 – Test C1.1_60, details with a bubble tag @time 17:30:07,02 on channel 1.

Fig. 48 represents the FFT of a period during which has not been recorded any bubble, vice versa Fig. 49 reports the FFT response of a period during which have been recorded a bubble. The " bubble tag" on Fig. 49 highlights energy variation at the frequency of 1550 Hz and 1730 Hz. This variation is due to the sound of a bubble.

With this method it is possible to recognize the energy variation and the characteristic frequency of the bubble generated from this orifice size.
During this test the microphone on channel 2 and channel 3 was set up with a low gain not sufficient to record this energy variation and the microphone on channel 4 and 5 was broken.

3.3.3 Analysis of the accelerometers and acoustic emission sensors data and interpretation

Dewesoft starting time corresponds to time t = 4312 during the LBE charging phase (started at t = 3906 and ended at t=6434). Considering the possibility to temporarily interrupt the recording, data are available starting from the initial steady-state conditions (LBE in S1A) from t = 6434 (SoT) and up to t = 11499 (EoT).

Fig. 50 and Fig. 51 show the elaborations of the acquisitions related to HTA (high temperature accelerometer), HSA (high sensitivity accelerometer) and AE (acoustic emission) sensors. In particular, Fig. 50 shows the trend over time of the effective RMS value, followed by Fig. 51 which displays the peak value of the measurements recorded by the sensors. Both values have been calculated in the time domain.

The analysis of the acquired data shows a correlation between the measurements recorded by the AE and HSA sensors, both installed on the upper flange of the S1A vessel, and subjected to influence of external events, such as the compressed air flow of the sensors cooling system. This correlation was evaluated by analyzing the start/stop signal of the sensor cooling system (AccelCooling) and checking the correspondence between the opening/closing times of the compressed air circuit within the acquisition of the sensors installed on the upper flange. Fig. 52 highlights these phenomena by narrowing the time window and changing the full scale of the signal amplitude.

Fig. 53 shows the time at which the maximum RMS value was recorded by the HSA sensor, presumably due to an external event such as the start of a compressor, equal to 0.70 g RMS. This time corresponds to $t_{dewesoft}$ = 01:28:01.

Considering the HTA sensor positioned inside the S1A vessel (Fig. 54), the acquisition shows an effective value of about 0.06 g RMS during the phase "S1A filled in steady state", and presents a maximum value of 2.3 g RMS at the time $t_{dewesoft}$ = 01: 20: 55. At the time t = 11507 (End of Test – EoT) corresponding to $t_{dewesoft}$ = 01: 59: 55, a value of 1.14 g RMS is recorded.

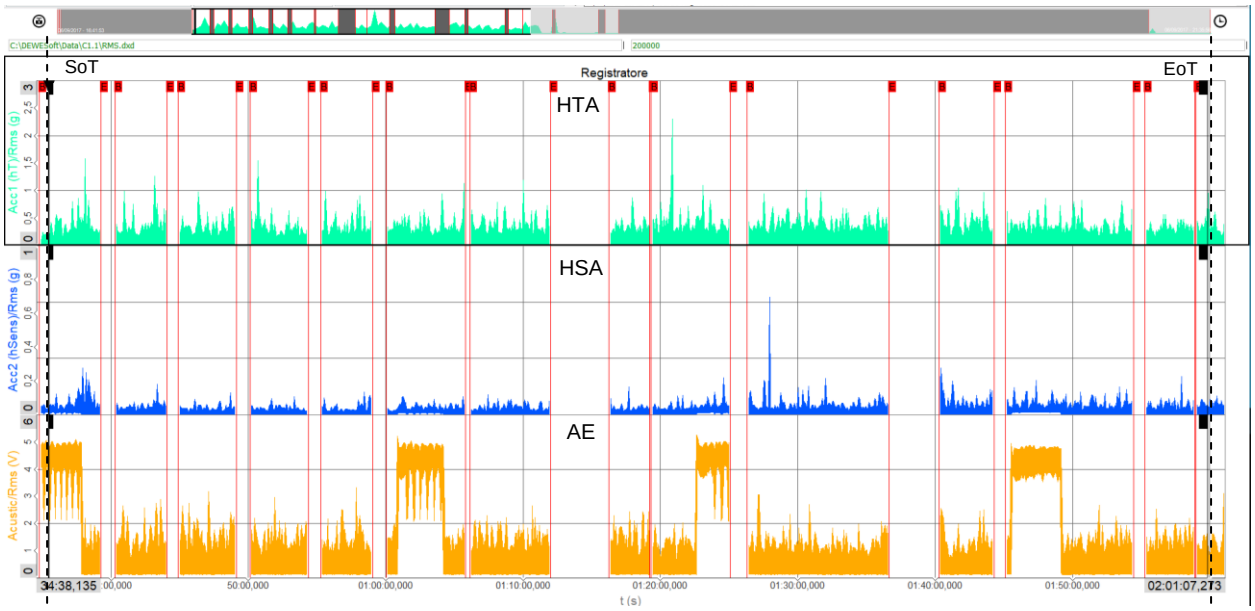

Fig. 50 – Test C1.1_60, HTA, HSA, AE time RMS trends.

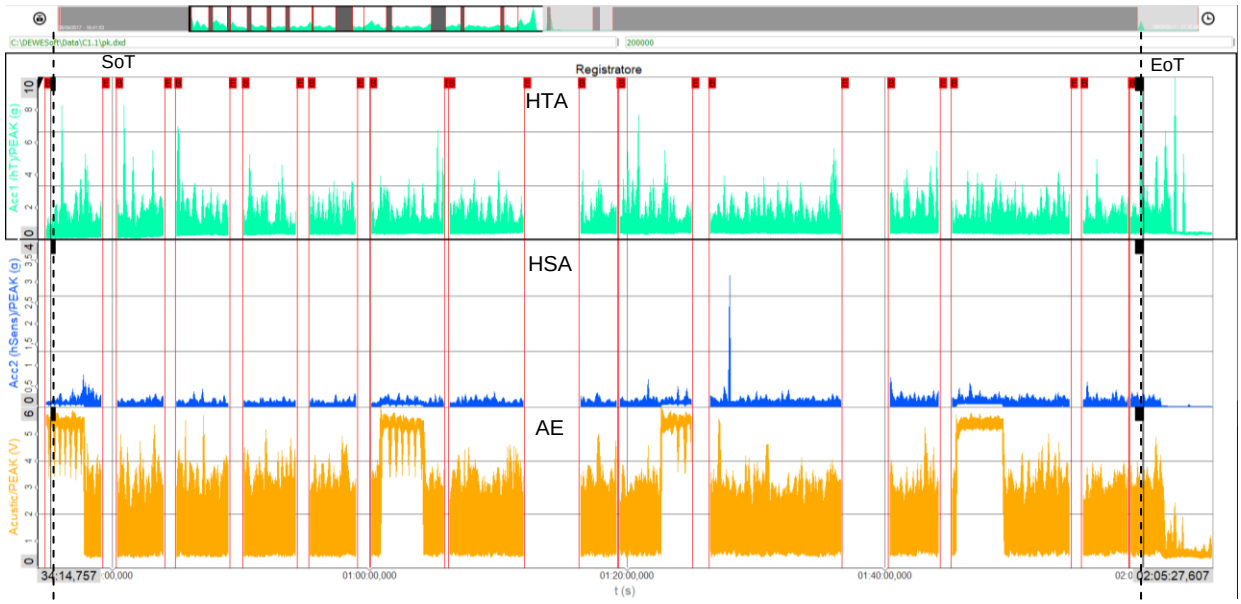

Fig. 51 – Test C1.1_60, HTA, HSA, AE time PEAK trends.

Fig. 52 – Test C1.1_60, HTA, HSA, AE time RMS trends.

Fig. 53 – Test C1.1_60, HTA, HSA, AE time RMS trends.

Fig. 54 – Test C1.1_60, HTA, HSA, AE time RMS trends.

4 Conclusions

The scope of this work was to present the experimental tests performed in LIFUS5/Mod3 facility, the acquired signals and the analysis performed.

The objective was fulfilled according the following rationale:

1) Description of the LIFUS5/Mod3 test section S1_A facility layout and features, the instrumentation installed, the implementation of the acoustic devices and to the alternative systems of accelerometers and acoustic emission, to detect the bubbles migration through the free level.
2) Description of the test matrix and reporting of one executed test.
3) Description and analysis of the acquired signals.

The objectives of the Test C1.1_60 were successfully achieved and the measurements acquired contribute to enlarge existing databases for SGTR events, providing an advancement in supporting the design of innovative HLM reactors.

The analysis of the thermo-hydraulic data permitted to characterize the leakage through typical cracks which can occur in pressurized tubes of steam generator.

The analysis of the data acquired by the Dewesoft system and recorded by the HTA, HSA, AE sensors highlighted that is possible to correlate the signals to the leakage, and to the rate of release. However, it has to be considered the installing position of instrument because the acquired signals are affected by external interferences.

List of references

[1] 7th FP THEME [Fission-2012-2.3.1] [R&D activities in support of the implementation of the Strategic Research Agenda of SNE-TP Nuclear Fission and Radiation Protection] – Annex I - "Description of Work"" Grant agreement no.:FP7- 323312, October 9, 2012.

[2] A. Del Nevo et al., “Deliverable D4.4 – SGTR Bubbles Characteristics”, MAXSIMA Project, April 2015.

[3] A. Del Nevo et al., “Deliverable D4.6 – Final Report on the Experimental Characterization of the Bubbles and Post Test Analysis”, MAXSIMA Project, June 2016.

[4] A. Pesetti, A. Del Nevo, N. Forgione, Experimental investigation of spiral tubes steam generator rupture scenarios in LIFUS5/Mod2 facility for ELFR, Proc. of 24th Int. Conf. on Nuc. Eng. (ICONE24), Charlotte, North Carolina, June 26-30, 2016, Paper No. ICONE24-60715, pp 1-11, DOI: 10.1115/ICONE24-60715

[5] A. Del Nevo, N. Giannini, A. Pesetti, N. Forgione, Experimental and Numerical Investigations of Interaction between Heavy Liquid Metal and Water for supporting the Safety of LFR Gen. IV Reactor Design, International Topical Meeting on Nuclear Reactor Thermal Hydraulics 2015, NURETH 2015, Vol. 9, 2015, pp. 7448-7461

[6] N. Giannini, et. Al., EC FP7 LEADER project: “Description of the configuration of LIFUS5/MOD2 facility”, Technical Report – L5-T-R-072, Rev.0, July 2014

[7] ISL Inc, “ RELAP5/MOD3.3 Code Manual Volume I: Code Structure, System Models, and Solution Methods “, Nuclear Safety Analysis Division, July 2003.